Aus der Klinik für Neurologie
der Medizinischen Fakultät Charité – Universitätsmedizin Berlin

DISSERTATION

TOWARDS AUTOMATED DEEP BRAIN STIMULATION PROGRAMMING

AUF DEM WEG ZUR AUTOMATISIERTEN PROGRAMMIERUNG DER TIEFEN HIRNSTIMULATION

zur Erlangung des akademischen Grades
Medical Doctor - Doctor of Philosophy (MD/PhD)

vorgelegt der Medizinischen Fakultät
Charité – Universitätsmedizin Berlin

von

Jan Roediger

Datum der Promotion: 23.03.2024

Table of contents

List of figures

List of abbreviations

ANTs	Advanced Normalization Tools
AUC	Area Under the Curve
CT	Computed Tomography
DBS	Deep Brain Stimulation
DiODe	Directional Orientation Detection
E-field	Electric Field
FEM	Finite Element Method
GLM	Generalized Linear Mixed Model
GPi	Globus pallidus internus
GUI	Graphical User Interface
MDS-UPDRS	Movement Disorder Society-Sponsored Revision of the UPDRS
MNI	Montreal Neurological Institute
MRI	Magnetic Resonance Imaging
PaCER	Precise and Convenient Electrode Reconstruction for DBS
PD	Parkinson’s Disease
ROC	Receiver Operating Characteristic
SoC	Standard of Care
STN	Subthalamic Nucleus
UPDRS	Unified Parkinson’s Disease Rating Scale
VAS	Visual Analogue Scale
VTA	Volume of tissue activated
VIM	Ventral intermediate part (of the thalamus)

Abstract

Background: Deep Brain Stimulation (DBS) of the subthalamic nucleus (STN) is an effective treatment option for patients with Parkinson's Disease (PD). To maximize treatment benefit, stimulation parameters need to be adjusted individually. Currently, this is performed following a trial-and-error approach, which is time-consuming, costly, and challenging for both patients and medical personnel. The recent introduction of directional electrodes has aggravated those difficulties, highlighting the need for more elaborate procedures to tailor DBS parameter selection to the individual patient. Recent studies suggested that the anatomical location of DBS electrodes could be used to predict beneficial stimulation parameters and guide DBS programming procedures.

Methods: We developed *StimFit*, a software to automatically suggest optimal stimulation parameters in PD patients treated with STN-DBS based on reconstructed electrode locations. The software was trained on a dataset of 612 stimulation settings (applied in 31 patients) to predict motor improvement and side-effect probabilities with respect to electrode location and stimulation parameters. Model performance was retrospectively validated within the training cohort and tested on an independent dataset of 19 PD patients. The predictive models were then embedded in a non-linear optimization algorithm to find parameter combinations which would maximize predicted therapeutic benefit. A graphical user interface was designed to allow for a streamlined use of *StimFit* and the software was made publicly available. Next, *StimFit* was prospectively applied in 35 PD patients in a double-blind, cross-over trial to assess whether motor benefit of *StimFit* stimulation parameters would be non-inferior to patients' standard of care treatment (SoC). Motor performance was evaluated according to the MDS-UPDRS-III under *StimFit* and SoC stimulation, randomizing the sequence of both conditions in a 1:1 ratio.

Results: Motor outcome predictions of the data-driven model integrated in *StimFit* correlated well with observed outcome within the training cohort ($R = 0.57$, $p < 0.001$) as well as in the retrospective test cohort ($R = 0.53$, $p < 0.001$). In our prospective clinical trial *StimFit* and SoC stimulation resulted in clinically significant average motor improvement of 43 and 48 %, respectively. Mean absolute difference of motor outcome between both conditions was -1.6 ± 7.1 (95% CI: [-4.0, 0.9]) establishing non-inferiority of *StimFit* at the pre-defined margin of -5 points ($p = 0.004$).

Conclusion: Beneficial stimulation parameters can be automatically derived from electrode location using data-driven approaches. Our results hold promise for more efficient and streamlined DBS programming procedures, but additional prospective studies are required to assess the effects of image-based DBS programming on non-motor domains and long-term quality of life.

Zusammenfassung

Hintergrund: Die Tiefe Hirnstimulation (THS) des Nucleus subthalamicus (STN) ist eine effektive Therapieoption zur Behandlung des idiopathischen Parkinson-Syndroms (IPS). Hierbei müssen die Stimulationsparameter individuell angepasst werden, was derzeit durch zeit- und ressourcenintensives Austesten erfolgt. Jüngste Studienergebnisse legen nahe, dass Informationen über die anatomische Lage der THS-Elektroden dafür genutzt werden könnten, vorteilhafte Stimulationseinstellungen zu identifizieren und somit die THS-Programmierung zu erleichtern.

Methoden: Wir entwickelten eine Software (*StimFit*), durch welche optimale Stimulationseinstellungen für Patient*innen mit STN-THS auf Basis ihrer individuellen Elektrodenlagen vorgeschlagen werden können. Hierbei wurde ein Trainingsdatensatz von 612 Stimulationseinstellungen (31 Patient*innen) genutzt, um THS-Effekte in Abhängigkeit von Elektrodenlage und Stimulationsparametern zu prädizieren. Vorhersagegenauigkeiten wurden retrospektiv innerhalb des Trainingsdatensatzes, sowie in einer unabhängigen Testkohorte von 19 Patient*innen quantifiziert. Die validierten Vorhersagemodelle wurden dann in einen Optimierungsalgorithmus integriert, um Stimulationseinstellungen mit maximalem (prädizierten) therapeutischen Benefit zu ermitteln. Der Algorithmus wurde in eine grafische Benutzeroberfläche eingebettet und öffentlich zugänglich gemacht. In einer doppelblinden cross-over Studie wurde *StimFit* dann prospektiv an 35 Patient*innen mit STN-THS angewandt. Hierbei wurden sowohl die von *StimFit* vorgeschlagenen, als auch die durch traditionelle Optimierungsverfahren ermittelten („Standard of Care“, SoC) Stimulationseinstellungen in randomisierter Reihenfolge eingestellt. Die therapeutischen Effekte der *StimFit*-Einstellungen wurden mittels des MDS-UPDRS-III quantifiziert und diesbezüglich auf Nicht-Unterlegenheit gegenüber dem SoC untersucht.

Ergebnisse: Die durch *StimFit* prädizierten motorischen Effekte korrelierten mit den empirischen Effekten innerhalb der Trainingskohorte ($R = 0,57$; $p < 0,001$) sowie in der retrospektiven Testkohorte ($R = 0,53$; $p < 0,001$). In der prospektiven Studie verbesserten sich die motorischen Symptome sowohl unter *StimFit*- als auch unter SoC-Stimulation (43 und 48 %). Der Summenscore des MDS-UPDRS-III unterschied sich statistisch nicht signifikant um -1,6 ± 7,1 (95% CI: [-4,0; 0,9]) zwischen beiden Stimulationskonditionen. Die Nicht-Unterlegenheit von *StimFit* konnte bei einer vordefinierten Grenze von -5 Punkten gezeigt werden ($p = 0,004$).

Schlussfolgerungen: Effektive Stimulationseinstellungen können anhand der Elektrodenpositionen durch automatisierte datengetriebene Algorithmen abgeleitet werden und somit die Optimierung der THS-Parameter erleichtern. Weitere prospektive Studien sind notwendig, um Langzeiteffekte und den Einfluss datengetriebener THS-Programmierungsmethoden auf nicht-motorische Domänen und die Lebensqualität der Patient*innen zu ermitteln.

1 Introduction

1.1 Subthalamic stimulation as a treatment for Parkinsons's Disease

A series of non-human primate and clinical studies in the late 1980s and early 90s, have led to the ground-breaking discovery, that high frequency electrical stimulation of specific subcortical structures can alleviate symptoms of movement disorders, especially those of Parkinson's Disease (PD). Namely, the ventral intermediate (VIM) part of the thalamus, the internal part of the globus pallidus (GPi) and – most importantly – the subthalamic nucleus (STN) were identified as targets for therapeutic neuromodulation to improve the cardinal features of PD – tremor, bradykinesia and rigidity.[1-5] The striking effects of subthalamic stimulation resulted in the approval of STN-DBS surgery as a treatment option for PD through the Food and Drug Administration and Conformité Européenne in 2001 – only six years after it was first bilaterally applied in three patients.[6] In the following decade five large randomized controlled studies were conducted (total n = 1,139), consolidating the initial findings by showing that on average patients' motor symptoms improved by 35% (according to part III of the Unified Parkinson's Disease rating scale, UPDRS-III), dopaminergic medication could be reduced by 37%, and – ultimately – disease related quality of life was improved by 21%.[7] Since then, advancements of surgical techniques and neuroimaging, along with hardware developments have steadily increased the risk-benefit ratio of the

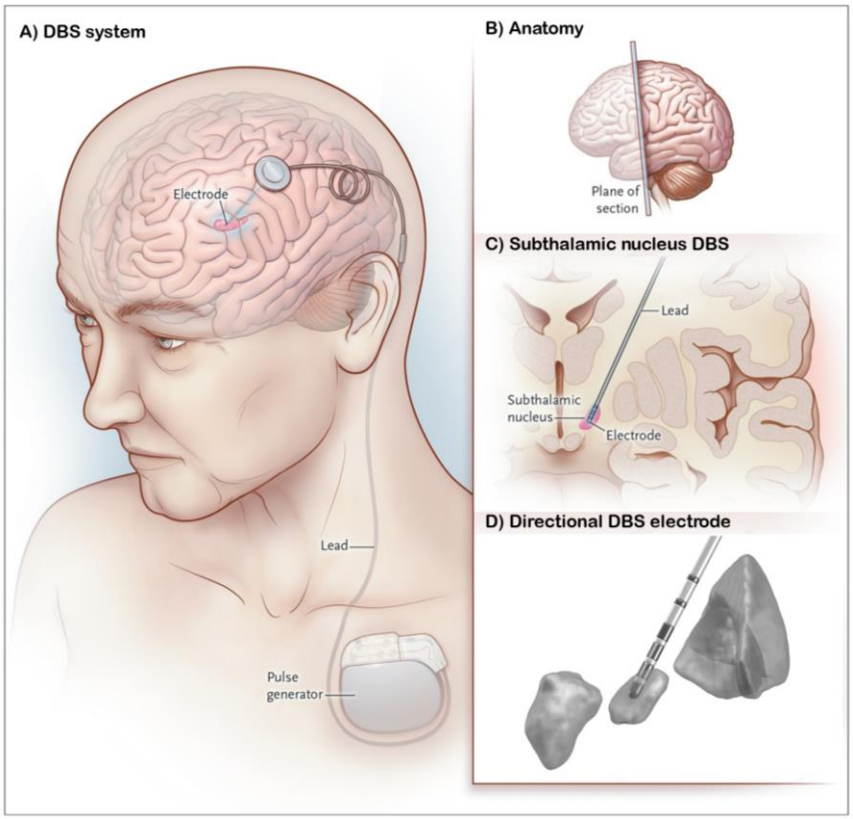

Figure 1: Deep Brain Stimulation. A) The DBS electrode targeted at the subthalamic nucleus is connected to a subcutaneously implanted pulse generator. B and C) Anatomical location of a STN-DBS electrode. D) 3D representation of an octopolar directional electrode with two segmented levels. Panels A to C adapted from Okun et al. 2012

therapy, allowing to successively widen its indication and establishing DBS as a fundamental treatment for PD.[8, 9] One of the most recent technical innovations was the introduction of directional DBS electrodes (**Figure 1D**).[10] Here, electric current can be applied across up to eight contacts independently. The tripartite segmentation of two contact levels allows to flexibly shape the electric field and can thereby help to precisely engage target structures, while avoiding stimulation of neighboring regions, which could potentially induce side-effects. This has shown to reflect in a widened therapeutic window compared to omnidirectional stimulation.[11, 12] *In silico* simulations have further suggested, that more complex DBS electrodes could in theory provide additional benefit by allowing to selectivity focus stimulation effects on specific target fibers.[13]

1.2 DBS parameter optimization – current strategies and limitations

However, in clinical practice, programming of DBS devices is performed manually by clinical trial-and-error. In other words, stimulation parameters are iteratively adapted by medical personnel based on therapeutic outcome or the occurrence of stimulation-induced side-effects. Despite the availability of multiple guidelines to streamline and facilitate parameter selection of clinical optimization procedures, following factors impose major limitations to this approach.[14, 15] First, therapeutic effects show a differential delay to stimulation onset.[16] More precisely, tremor improvement in most patients is almost immediately visible after stimulation is turned on, whereas 90% of the maximum effects on rigidity and bradykinesia are reached after 15 to 30 minutes of stimulation and axial effects are showing an even slower response. Vice versa, wash-out of stimulation effects is observed on even larger timescales but with similar succession of different motor symptoms. This leads to a complex interplay of carry-over effects when testing multiple settings, making it extremely challenging to reliably judge the outcome of varying stimulation parameters within a single programming session. Hence, parameter optimization should ideally be conducted over the course of several days to evaluate the clinical effects of parameter adjustments after sufficient wash-in periods. However, comparability between stimulation

settings can then be impeded by symptom fluctuations and medication adjustments, which need to be applied in parallel to optimize treatment benefit. To achieve a steadier baseline of motor symptoms, Off-medication testing, especially within the scope of an initial "monopolar review" is regularly performed **(see panel "Monopolar Review")**. This, on the other hand, can be experienced as very strenuous for patients and outcome evaluations are therefore – in addition to abovementioned carry-over effects – often blurred by patient fatigue. Taken together, only a few settings can be reliably probed by clinical testing, contrasting the overwhelming number of more than 10^{10} possible stimulation settings in currently available octopolar electrodes. Hence, technical possibilities of modern DBS systems cannot be exhausted in clinical practice. Moreover, this imposes a serious constraint on potential technical innovations, since current clinical programming strategies would not allow to take advantage of the theoretical benefits of more complex systems. Lastly, clinical optimization strategies are highly time-consuming and require well-trained medical personnel as well as specialized centers, imposing a large economic burden and limiting the number of patients which can receive high-quality post-operative care following DBS surgery.

Monopolar Review
Modern DBS devices allow to distribute electric current independently across up to eight contacts at the tip of the electrode. A "monopolar review" is performed to identify beneficial contacts by individually selecting each contact as a cathode and iteratively evaluating DBS effects with increasing stimulation amplitudes while other parameters like pulse-width and frequency are kept constant. This way a therapeutic window can be identified for each contact. It is defined as the range between the minimum stimulation amplitude necessary to elicit therapeutic effects and the amplitude at which stimulation-induced side-effects are observed.

1.3 Imaging-guided DBS programming

Algorithms which integrate biomarkers predictive of stimulation outcome could provide a possible solution to the current limitations of DBS programming.[17-21] A clear link between electrode location, stimulation parameters and clinical outcome has been established within recent years across various DBS targets and diseases.[22-28] More specifically, numerous studies have shown that, based on electrode reconstructions and stimulation parameters, clinical outcome could be predicted in out-of-sample data, suggesting that electrode location could be used as a predictive feature to derive optimal stimulation parameters in individual patients. Importantly, in most of these studies DBS-electrodes were

reconstructed based on routinely acquired perioperative neuroimaging data (pre-operative magnetic resonance imaging (MRI) and postoperative computed tomography (CT)).[29, 30] From a practical perspective this makes a potential implementation of imaging-guided DBS programming in clinical routine especially feasible, since no additional data acquisition or hardware would be required. Previous approaches to integrate neuroimaging data in DBS programming procedures relied on visualizing the anatomical regions directly affected by stimulation.[21, 31-33] In detail, after reconstructing DBS electrodes and specifying stimulation parameters, a volume of tissue activated (VTA) is being estimated in relation to the patients' brain anatomy **(Figure 2)**.[34-38] This way, DBS settings can be probed *in silico,* aiming at maximally engaging target regions, while avoiding stimulation of anatomical structures that could potentially induce side-effects. While this strategy can provide a first impression of potentially beneficial stimulation settings, optimizing DBS treatment this way remains challenging for following reasons. First, DBS parameters need to be manually adjusted within the software. Considering the overwhelming amount of possible stimulation settings, manually identifying optimal parameter combinations this way remains time-consuming. Second, current software solutions do not provide a clear definition of target regions or regions of avoidance. More specifically, the dorsolateral STN has been identified as the optimal target for suppression of akinesia and rigidity in PD patients but the exact volume that needs to be covered by the VTA is not clearly defined.[24, 39, 40] The same problem exists for stimulation-induced side-effects. Stimulation of the posterior region of the internal capsule – for example – is linked to tonic motor contractions but a clear specification of this region or the amount of overlap that could be tolerated before eliciting clinically relevant side-effects is

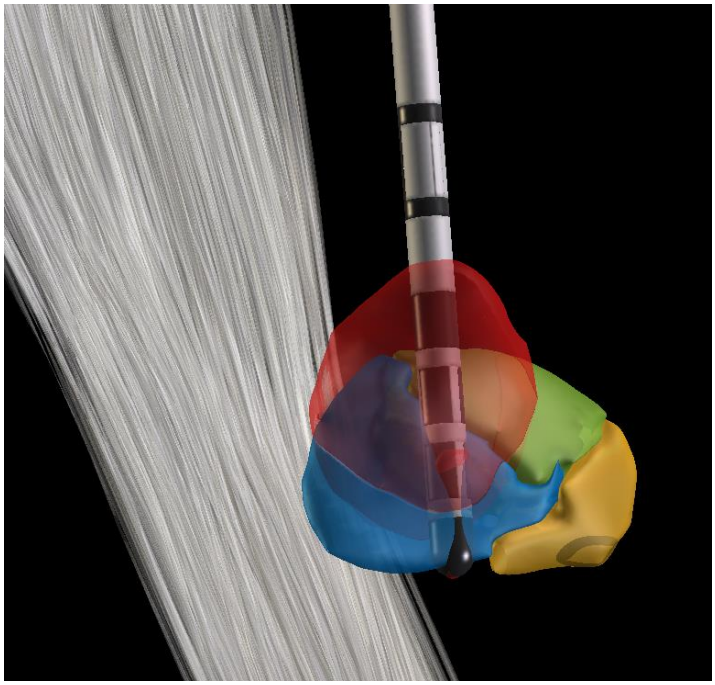

Figure 2: Volume of tissue activated in respect to patients' anatomy and electrode placement. Sensorimotor (blue), associative (green), and limbic (yellow) regions of the subthalamic nucleus (Acolla et al <REF>) shown in respect to the patients DBS electrode. Using a simplified "bottom up" model of neuronal activation the region affected by a certain stimulation setting (contact 7, 3mA, 60µs, 130Hz) is shown in red. Anatomy-guided DBS programming aims at identifying settings which maximally engage target regions, while minimizing stimulation of regions which could induce side-effects (e.g. corticospinal tract shown in white).

not provided.[41] Last – and most importantly, not only the target regions and regions of avoidance remain ill-defined, but also the VTA itself represents a vague metric to estimate the regions affected by DBS as described in the following section.

1.4 Predictive models for DBS

1.4.1 “Bottom-up” models

The VTA is a biophysical model of neuronal activation. While nowadays heuristic approximations are widely used in the field of DBS research, it was originally based on simulations of axon-cable models, which use differential equations to approximate the electrical characteristics of neurons (obtained from cellular experiments) to predict their response to the electric field generated by a DBS impulse.[42-44] The model is used to binarize brain tissue as being “activated” if action potentials are elicited *in silico* within this region. The simplicity of visualizing “active” vs “inactive” tissue this way seems practical, not only for clinical, but also for scientific use. Multiple studies have applied heuristic approximations of these models to map stimulation outcome to anatomical brain regions (probabilistic mapping), in order to identify local stimulation “sweet-spots“ or connected brain regions, which are linked to optimal therapeutic outcome.[22-24, 26, 45] This has shed light onto the anatomical structures involved in therapeutic neuromodulation across various diseases and opened up new avenues for novel stimulation targets.[46-48] However, visual stimulation feedback provided by current (commercial or non-commercial) programming software should be interpreted with caution to avoid misinterpretation – and ultimately – suboptimal patient treatment for following reasons: First, the underlying biophysical models are susceptible to parameter modifications like ion-channel properties, fiber orientation and axon diameters, most of which are unknown in the individual target region.[49-51] Second, biophysical “bottom-up” models do not only lack (or neglect) important knowledge about the functioning of the human brain, but whether or not behavioral effects can be predicted this way remains controversial in principle. The reductionist belief that – given enough knowledge and information about the causal relationships and the state of a human brain, behavior could be explained based on the laws of physics – is omnipresent and appealing among neuroscientists but highly debated in other fields of science and philosophy.[52] The idea that higher-order observations exclusively obey lower-order laws, has always been challenged and is especially questionable in complex and nonlinear

systems like the human brain, where phenomena at different hierarchical levels reciprocally act upon each other, generating a behavior of the system which would not be explainable by the properties of its components alone (i.e. *emergence*).[53, 54] Despite the valuable contribution of computational neurosciences to understand and capture essential laws of the nervous system at different levels of organization (e.g. single-neuron, synapses, sensory/motor subdomains, cognition and behavior), cross-sectional models (from single-cells to human behavior) have yet to be established. In conclusion, biophysical models can – if applied carefully – be a powerful tool to gain insights into the mechanism of action and anatomical target structures in therapeutic neuromodulation, but may not represent the most reasonable approach if the objective is to accurately predict clinical outcome to optimize treatment benefit.

1.4.2 “Top-Down” models

On the other end of the spectrum, there are purely data-driven models, which link input-output relations without necessarily reflecting biophysical mechanisms. Today’s choices of these supervised learning algorithms are manifold ranging from classical regression models to support vector machines and artificial neural networks. In the field of DBS these applications have been suggested to quantify symptom severity, guide DBS-implantation or to predict surgical complications.[55-57] Further, many studies have successfully applied data-driven models for real-time adaptation of DBS to electrophysiological or kinematic features.[58-61] Most models in DBS neuroimaging however, strongly rely on “bottom-up” VTA estimations and out-of-sample predictions have shown to be susceptible to varying statistical implementations.[62] This may be the reason why – despite the urgent need for streamlined DBS programming – these models have not yet been leveraged to predict optimal stimulation parameters in individual patients or validated prospectively in randomized controlled trials.

1.5 Model implementation and study aims

Aiming at overcoming these limitations, we developed a novel data-driven approach, to predict therapeutic and adverse stimulation effects based on electrode location and stim-

ulation parameters.[63] Using a hybrid approach between bottom-up modeling of the physical effects induced by DBS (E-field modeling) and top-down supervised learning (voxel-based ensemble model, described in detail in section 2.2.3), the model was trained to predict improvement of akinetic-rigid symptoms and tremor as well as probabilities of stimulation-induced side-effects. In the scope of the first dissertation study the model was cross validated within the training cohort as well as retrospectively applied on an independent test cohort. An additional validation was performed by comparing the optimal stimulation location ("sweet-spots") according to our model to previously published literature results. These retrospective anatomical and statistical validations were performed to ensure that the model allowed to reliably predict DBS outcome in out-of-sample data. However, the overall aim of this study was to develop an algorithm which could suggest *optimal* stimulation parameters in novel patients. In the next step, the trained model was therefore embedded in a mathematical optimization procedure, to iteratively adjust stimulation parameters *in silico* in order to converge to a setting which would maximize predicted treatment benefit. In other words, the optimizer could – based on out-of-sample electrode locations – suggest stimulation settings with maximum predicted motor benefit, while minimizing the risk of stimulation-induced side-effects. Within the retrospective test dataset, the settings suggested by the algorithm were compared to clinically derived stimulation settings to assess whether clinical settings, which were similar to algorithmic suggestions, were associated with better stimulation outcome. Finally, the algorithm *(StimFit)* was integrated in a graphical user interface for a clear and streamlined use. The code was made openly available at https://github.com/JRoediger/StimFit. In the second dissertation study stimulation parameters suggested by *StimFit* were then prospectively applied in 35 PD patients and clinical outcome was compared to patients' standard of care treatment (SoC) in a randomized double-blind cross-over design.[64]

2 Methods

2.1 Datasets

85 PD patients who underwent bilateral subthalamic DBS at Charité – Universitätsmedizin or University Hospital Cologne were included for training and cross-validation (n = 31)[11, 24], retrospective (n = 19)[20] as well as prospective (n = 35)[64] evaluation of the algorithm. At both centers a thorough multidisciplinary evaluation process preceded stereotactic surgery to ensure optimal patient selection. Additionally, intraoperative microelectrode recordings as well as macrostimulations were regularly performed to optimize lead-placement. Multiple high-quality MRI-sequences (T1, T2) were obtained preoperatively for stereotactic planning and to exclude neurological comorbidities. Postoperatively thin-layer CT scans were acquired to rule out major surgical complications like bleeding or lead displacement. These perioperative imaging data were used to reconstruct electrode locations in relation to patients' individual anatomy using Lead-DBS as described in section 2.2.1 Electrode reconstruction.[29, 30]

A total of 828 stimulation settings applied on 154 electrodes were included in the analyses along with their corresponding behavioral effects. All assessments were conducted after patients underwent withdrawal of dopaminergic medication for >12 hours. Subjects included in these studies gave written informed consent and all studies were approved by the local ethics committee to be in accordance with the declaration of Helsinki.

2.1.1 Training data (Dissertation study I)

Data of two previously published cohorts were used for training and cross-validation of the algorithm.[11, 24] Briefly, the first cohort was acquired for a study conducted at the University Hospital of Cologne to investigate the optimal stimulation location in PD patients. Using two independent test cohorts this study was the first to predict clinical improvement of parkinsonian motor symptoms based on local DBS effects, hence paving the way for the projects conducted within the scope of this dissertation. The second cohort was prospectively collected within the scope of a study carried out by Dembek & Reker et al. to compare the effects of directional and circular stimulation, thus contributing to converging evidence showing a therapeutic advantage of directional DBS.

Across both studies 31 PD patients underwent standardized monopolar review examinations according to the following protocol: Electrodes were examined by applying current on each contact with increasing amplitudes up to five milliampere or until limiting side-effects occurred. The order of stimulation contacts was randomized, and frequency and width of stimulation pulses were set to 130 Hz and 60 µs. At each one milliampere increment, parkinsonian motor symptoms of the contralateral upper extremities were assessed according to items 20 to 23 and 25 (akinesia, rigidity, and tremor) of the Unified Parkinson's Disease Rating Scale (UPDRS) part III. Motor improvements were calculated as relative change compared to OFF-stimulation impairment. Additionally, the occurrence of non-transient side-effects was documented at each step. This way a total of 612 stimulation settings on 46 electrodes (25 Medtronic 3389, 20 Boston Scientific Vercise™ directional, one Boston Scientific linear 8-contact) were evaluated.

2.1.2 Retrospective test data (Dissertation study I)

Test data were previously collected from 19 patients who enrolled in a study investigating the feasibility of algorithm-guided programming based on kinematic feedback.[20] In this study Wenzel et al. used an algorithm, which – based on kinematic data of wearable finger sensors – suggested different stimulation parameters throughout the programming session until convergence to a final solution. These settings were then evaluated according to the UPDRS-III in a double-blind cross-over design in comparison to patients' standard settings derived from clinical programming. To assign stimulation effects to each electrode (32 Boston Scientific Vercise™ directional, 6 Boston Scientific linear 8-contact), UPDRS-III items of the contralateral side of the body were summed (hemi-body score) and improvements relative to Off-stimulation baseline were calculated.

2.1.3 Prospective test data (Dissertation study II)

A prospective randomized double-blind cross-over trial was carried out to evaluate stimulation effects of *StimFit* settings in comparison to standard of care (SoC) treatment.[64] 35 PD patients bilaterally implanted with directional octopolar leads (64 Boston Scientific Vercise™ directional, 6 Medtronic SenSight™) were recruited. Inclusion criteria were the diagnosis of PD treated with STN-DBS using directional octopolar electrodes. Patients underwent DBS surgery between three months and three years before recruitment and

DBS parameter optimization was carried out according to the standard clinical practice at Charité Universitätsmedizin. This included monopolar review examinations **(see panel "Monopolar Review")**, titration of stimulation parameters and adaptation of dopaminergic medication during several in- and outpatient visits at specialized facilities. *StimFit* stimulation parameters were obtained according to the pipeline described in section 2.2.7. Resulting SoC settings had to have remained unchanged for a minimum of four weeks before study participation. Exclusion criteria were cognitive impairment, neuropsychiatric symptoms, severe cerebral atrophy, the inability to undergo overnight withdrawal of dopaminergic medication or surgical complications like bleedings, infections of the DBS system or re-implantation of DBS electrodes. Patients were asked to withdraw dopaminergic medication overnight and remained in Off-medication condition during the whole study examination. The study was approved by the local ethics committee (EA2/117/19) and registered at the German Register for Clinical Trials (https://www.drks.de, Study-ID: DRKS00023115).

2.2 Data analysis

2.2.1 Electrode reconstruction

DBS electrodes were reconstructed using the default pipeline integrated in the Lead-DBS software **(Figure 3)**.[29, 30] In detail, rigid (within-patient) registration of preoperative MRI sequences was performed using SPM12.[65] Similarly, postoperative CT images were co-registered using Advanced Normalization Tools (ANTs).[66] Afterwards, to allow for analyses across patients, images were warped to Montreal Neurological imaging (MNI-152) template space.[67] This spatial normalization was performed using the non-linear Syn registration approach as implemented in ANTs. Additionally, a final linear registration called "Brain shift correction" was applied to account for potential misalignments between pre- and postoperative images caused by air entering the skull during DBS surgery introducing a displacement in the target region.[68] All registration steps were visually inspected and re-run, if necessary, but no manual corrections (e.g. using fiducial registration in 3D Slicer or the "warp-drive" tool developed by Oxenford et al[69]) were performed, to avoid introducing inhomogeneous distortions which might negatively affect the prediction model described in section 2.2.3 Predictive model. Finally, electrode positions and their rotations were reconstructed according to the electrode artefact visible in the postoperative CT

scans. This was done using the PACER and DiODe algorithms and was manually corrected after visual inspection if necessary.[70, 71]

2.2.2 Electric field simulation

Modeling the electric field (E-field) in the target region is an essential step in many studies investigating the biophysical interrelations of DBS. The modeling pipeline implemented in Lead-DBS was adapted to estimate the electric field generated by specific stimulation settings in a time-efficient manner **(Figure 3)**. This pipeline uses the finite element method (FEM) to estimate the E-field in the target region for a given combination of stimulation parameters. In detail, the pipeline starts by constructing a three dimensional mesh, composed of tetrahedral elements which were generated using "TetGen".[72] Conductivity values are then assigned to each of these elements (contact material = 10^8 S/m, insulating material = 10^{-16} S/m, neural tissue = 0.2 S/m). Next, the SimBio/Fieldtrip pipeline was used to estimate voltage gradients at each compartment. The amplitude applied to the active contact was introduced as a cathodal boundary condition and the outer surface of the modeled area served as an anode (since only monopolar stimulation settings were used throughout this study). Finally, voltage gradients were re-sampled in MNI space to a standard 100 x 100 x 100 grid with a 0.4 mm iso-spacing, centered at the dorsolateral STN.

Estimating the E-field of one stimulation setting this way took approximately two minutes on a local workstation. To speed up computational time the additive properties of the E-field were taken advantage of.[73] Specifically, once electrode localizations were completed, FEM simulations were conducted for each contact with a fixed amplitude of five milliampere. Resulting E-fields were saved in the patient folder and used as templates to

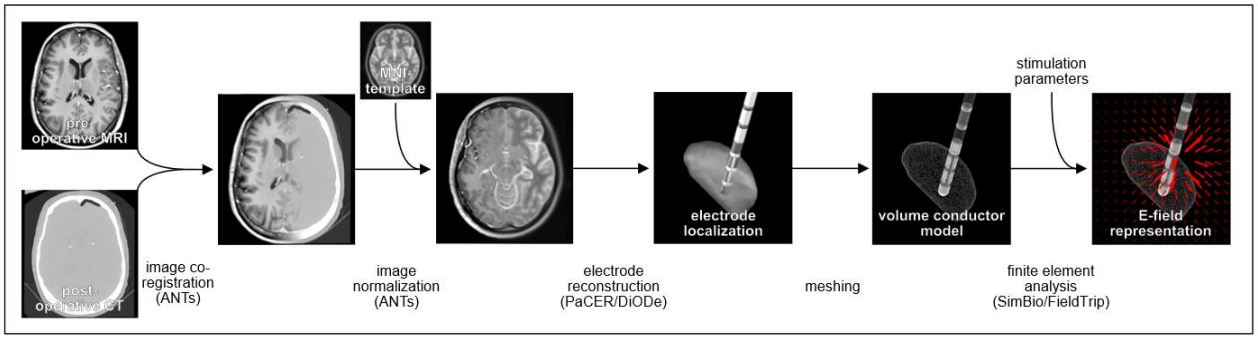

Figure 3: Pre-processing pipeline. After co-registration of perioperative neuroimaging data and normalization to MNI-space, electrode artefacts were used to localize DBS electrodes in respect to the patients' neuroanatomy. A volume conductor model was generated allowing to estimate E-field gradients in respect to specific stimulation parameters. Figure adapted from Roediger et al. 2022

compute E-fields of other stimulation configurations (including multi-contact stimulation) without the need of computationally expensive FEM simulations. In detail, scalar multiplication and superposition was applied to E-field templates to obtain E-field simulations of novel stimulation settings. Formally, E-fields E_{new} generated by a stimulation amplitude a distributed with a relative proportion w across contacts n were computed as:

$$E_{new} = \sum_{n}^{N} T_n * w_n * \frac{a}{a_{n0}}$$

Where N is the total number of contacts, T_n is the pre-computed E-field template and a_{n0} is the stimulation amplitude used for generating the template T_n, which was set to 5 mA. This way computational time to simulate an E-field could be reduced by a factor of ~10,000 to approximately 15 ms. To validate this approach, spatial correlations between E_{new} and corresponding FEM-based simulations were calculated for a randomly selected sample of patients and stimulation settings and revealed almost identical solutions ($R > 0.99$, $p<0.001$).

2.2.3 Predictive model

2.2.3.1 Vector field model

E-field simulations were used as a model input to predict behavioral effects. Therefore, E-field vectors were sampled at 125,000 voxels of an isometric size of 0.8 mm in the target. An ensemble modeling approach was applied where each voxel could “vote” on the final prediction. Individual voxel predictions were based on the magnitude and directionality of the E-field vector at this location. In order to represent directionality, each voxel was radially divided into 26 sectors of similar size and shape (see **Figure 4** for a 2-dimensional illustration). Within each voxel an E-field vector would – depending on its directionality – fall inside one of these sectors. A sector represents the smallest unit of the ensemble and contains the statistical model which links the magnitude of the E-field vector to the behavioral outcome. If – across all training data – an association between the voltage gradient and behavioral effects was only present if the gradient was oriented along a specific direction, the model of the sector representing this direction could predict

stimulation outcome, while the models of other sectors within this voxel would perform poorly. In other words, the predicted outcome of a voxel would differ depending on the directionality of the E-field vector at that location. Linear mixed models (LMEs) were used to model the relationship between vector magnitude and stimulation outcome within a sector. To estimate the probabilities of side-effect occurrence a logit link function was implemented to model the relationship between vector magnitudes and side-effects as a binary response variable (logistic regression). Further, the model needed to be able to account for the nested structure of the data (multiple measures per electrode). “Electrode ID” was therefore introduced as a “random effect” (random slope and random intercept) in our model. Up to this point the section described how within each of the 125,000 voxels stimulation outcome was modeled in respect to the magnitude and directionality of the E-field vectors at each of these locations. In the next step these models needed to be combined to a final ensemble model. Importantly, some voxels might quite accurately predict stimulation outcome while others perform badly and introduce noise to the ensemble vote. The “certainty” of an outcome prediction can be expressed as a probability density function and a probabilistic ensemble prediction was obtained by averaging across the probability density functions of all voxel predictions.

In summary, using the cohort described in section 2.1.1, we trained a model to predict therapeutic effects and side-effect probabilities of stimulation settings based on the properties of the E-field in the target region. This allowed us to estimate acute stimulation effects of varying electrode locations, geometries, and active contact configurations across different behavioral effects.

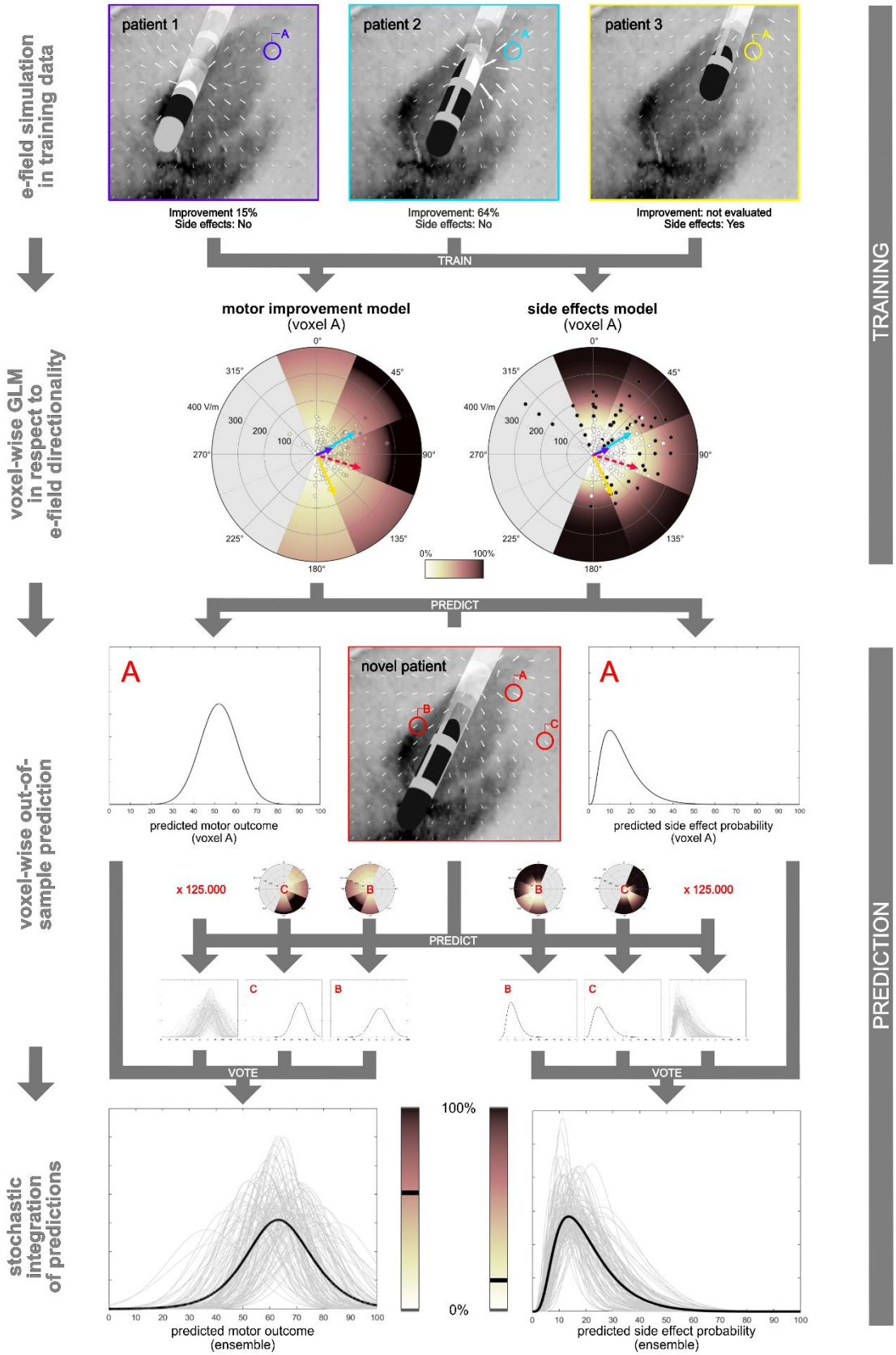

Figure 4: Vector field model. According to the pre-processing pipeline depicted in Figure 3, E-fields are being generated for each stimulation setting of the training cohort. E-field gradients are sampled at 125,000 anatomical locations and at each location a GLM is trained to predict stimulation outcome (motor and side-effects) based on vector magnitudes and directionalities. Differential effects of vector directionalities are captured by radially dividing each voxel in different segments, which is depicted as a 2D representation (polar plots). DBS outcome of novel stimulation settings can then be predicted at each voxel individually and stochastically integrated for final ensemble predictions. Figure from Roediger et al. 2021

2.2.3.2 Statistical validation

Model performance within the training cohort was assessed applying four-fold cross-validation. In detail training data was divided in four sets of approximately equal size and outcomes of each set were iteratively predicted after training the model on the remaining three sets. Motor outcome predictions were assessed by calculating Pearson's correlation coefficient between predicted and observed improvements across patients. Model performance regarding predictions of side-effect probabilities was quantified by calculating the area under the receiver operating characteristic curve (ROC-AUC). Additionally, model performance was evaluated on an independent test cohort (section 2.1.2), again using Pearson's R between predicted and observed motor improvements. Noteworthy, in contrast to the training dataset evaluation, side-effect predictions could not be tested within this cohort, since none of the chronic stimulation settings applied here elicited side-effects.

2.2.3.3 Anatomical validation

In order to identify the optimal stimulation target (sweet-spot), model predictions were evaluated at different arbitrary stimulation sites. Specifically, a two milliampere stimulation was simulated, applied on a circular contact at each of the aforementioned 125,000 locations in MNI space. Motor improvements and side-effect probabilities were predicted at each of these locations. This allowed to identify regions which would – according to the model – lead to optimal motor response as well as regions with an increased likelihood to elicit side-effects. Results were then visualized in MNI space and compared to previous literature findings.

2.2.4 Nonlinear optimization

Up to this point a method to predict therapeutic and adverse effects of STN-DBS based on electrode location was developed and validated, harnessing a voxel-wise ensemble model. The overall aim of this project, however, was to establish an algorithm which can identify *optimal* stimulation parameters based on electrode location. Importantly, modern DBS devices allow to distribute electric current independently across contacts allowing for $> 10^{10}$ combinatorial possibilities on octopolar electrodes. Thus, a complete exploration of all possible settings would be unattainable, despite applying various techniques to

improve computational time (section 2.2.2). Therefore, a nonlinear optimization algorithm was implemented to identify optimal stimulation settings in a reasonable amount of time. The vector-field model **(Figure 4)** described in section 2.2.3 represents the core function of the solver to compute predicted motor improvement and side-effect probabilities given a certain distribution of electric current across contacts (input vector). Iteratively, the solver adjusts the values of the input vector to maximize the objective function (motor improvement). Further, a maximum side-effect probability is defined by the user (nonlinear constraint). According to the technical restrictions of the DBS device additional constraints can be applied to define minimum and maximum current per contact (lower and upper bounds) as well as the maximum total current (linear inequality constraint) across the input vector. Thus, taking into account the outcomes and constraint violations of previous iterations, adjustments to the input vector are being made until the solver converges to a final solution. Formally, according to MATLAB® syntax the solver *fmincon* was defined as:

$$[I_{opt}, M_{opt}] = fmincon(f_{obj}, I_0, lcon, vlcon, \sim, \sim, Ib, ub, f_{nlc})$$

Here, I_{opt} described the final solution of electric current applied on each contact to achieve the predicted motor improvement M_{opt}. f_{obj} represents the objective function to calculate motor improvement. Nonlinear constraint violations (side-effect probabilities greater than the pre-defined threshold) are calculated by the function f_{nlc}, linear inequality constraints are defined by *lcon* in respect to the input vector *vlcon* (e.g., maximum total current across all contacts) and *lb* and *ub* define the lower and upper bounds (maximum current per contact). Finally, I_0 is the stimulation setting used as a starting point for the solver (details described in section 2.2.5).

Importantly, as shown in **figure 12**, anatomical sweet-spots for tremor and akinetic-rigid symptoms were segregated in our model. This implies that stimulation settings which are optimal to suppress akinesia and rigidity differ from the settings which lead to a maximum suppression of tremor. Subsequently, optimal stimulation settings differ from patient to patient depending on the individual symptom profile. This aspect was implemented in the algorithm by allowing the user to define the degree to which tremor should be accounted for in respect to akinetic-rigid symptoms on a continuous spectrum from 0 % to 100 %. With each iteration the algorithm separately predicts akinetic-rigid improvement as well

as tremor before combining the results to a final motor improvement score according to the user-defined weight. Formally this can be expressed as:

$$f_{obj} = w * f_{trem} + (1 - w) * f_{akinrig}$$

Where, f_{trem} and $f_{akinrig}$ describe the functions to calculate tremor and akinetic-rigid improvements which are then combined to the objective function f_{obj} according to the user-defined weight w (with $0 \leq w \leq 1$). The impact of adjusting w on the suggested contact selection is visualized in **figure 12**.

2.2.5 Improvement of speed and performance

In summary, to obtain a suggested optimal stimulation setting, the solver iteratively changes the simulated stimulation settings until pre-defined stopping criteria, such as the changes of predicted outcome in previous iterations (function tolerance) or adjustments made to the input vector (step tolerance) are fulfilled. In each iteration outcome predictions need to be computed applying the vector field model (section 2.2.3) based on E-field simulations. This iterative process is computationally demanding, and several measures needed to be taken to avoid excessive computational time and ensure that the model converges to an optimal solution.

First, complex 'hilly' objective functions impose the risk of the optimizer stopping at a local instead of the global minimum. A multi-start strategy was therefore implemented, initiating multiple runs of the solver with different starting points, hence increasing the chance to find the global optimum with each individual run. To minimize the additional computational costs caused by this measure, we implemented the option to carry out multiple runs in parallel. Next, selecting starting points close to the optimal solution further increases performance and speed of the solver. This was done by simulating a "monopolar review" before running the optimizer. In detail, a grid-search was carried out, calculating motor improvements and side-effect probabilities of monopolar stimulation settings on each contact with increasing stimulation amplitudes. Optimal monopolar solutions were then identified for each contact and passed to the optimizer as starting points. This way a total of ~10,000 vector field calculations needed to be executed to obtain suggestions for optimal stimulation setting bilaterally.

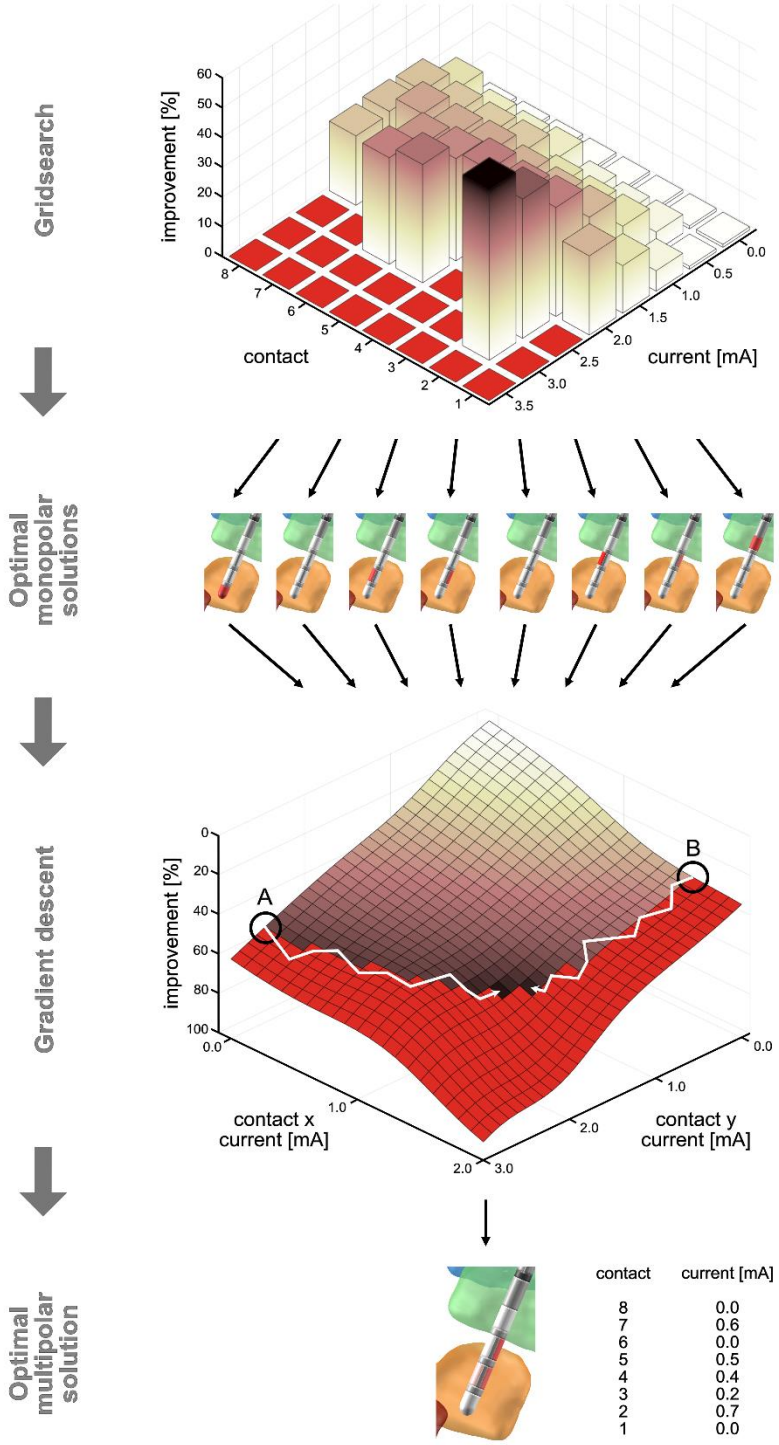

Figure 5: Optimization procedure. To identify optimal multi-contact configurations in a time-efficient manner a two-step optimization procedure was established. First, analogously to clinical "monopolar reviews" a grid-search was carried out, predicting motor improvements and side-effect probabilities of monopolar stimulation settings. Solutions in which predicted side-effect probabilities exceed the pre-defined threshold are discarded and shown in red. In the second step, optimal monopolar solutions are used as start points for a gradient descent algorithm to identify optimal multi-contact configurations. Again, solutions which exceed the side-effect threshold are discarded (nonlinear constraint) and represented in red. Figure from Roediger et al. 2021

However, bearing in mind that each vector field calculation required an E-field simulation as well as up to 125,000 predictions on a voxel-segment level, efficiency was especially important at this scale. This was addressed in two ways. First, as described in section 2.2.2, E-fields were obtained by exploiting their additive properties to avoid FEM-based simulations. This reduced the computational time for a single simulation from ~150 to ~0.015 s. Second, instead of iteratively solving GLMs at each voxel, millions of GLM solutions were pre-computed and stored in memory space. Thus, predictions could be obtained by identifying the best-matching pre-computed solutions leading to a reduction of computational time from ~600 to 0.35 s. Taken together, the abovementioned measures allowed to obtain stimulation suggestions bilaterally in ~50 min.

All computational work was carried out with MATLAB 2020a (The MathWorks Inc., Natick, Massachusetts, United States) on a local workstation with an AMD Ryzen 7 3600Hz 8-Core Processor and 64 GB RAM.

2.2.6 Graphical User Interface

Using MATLAB® AppDesigner the software was embedded in a Graphical User Interface (GUI) for a clear and streamlined use **(Figure 6)**. The App allows to select single patient folders or batch process multiple patients at once. Maximum side-effect probabilities as well as the degree to which tremor should be accounted for can be adjusted from 0 to 100 %. Additionally, optimizer settings can be adjusted in a separate popup window and saved allowing to evaluate the impact of different solver options, constraints, stopping criteria and parallelization on speed and outcome of the computations. Along the same lines, progress and results of optimizer iterations can be tracked and visualized live or post-hoc for a detailed analysis. The Software was named *StimFit* and is openly available under https://github.com/JRoediger/StimFit.

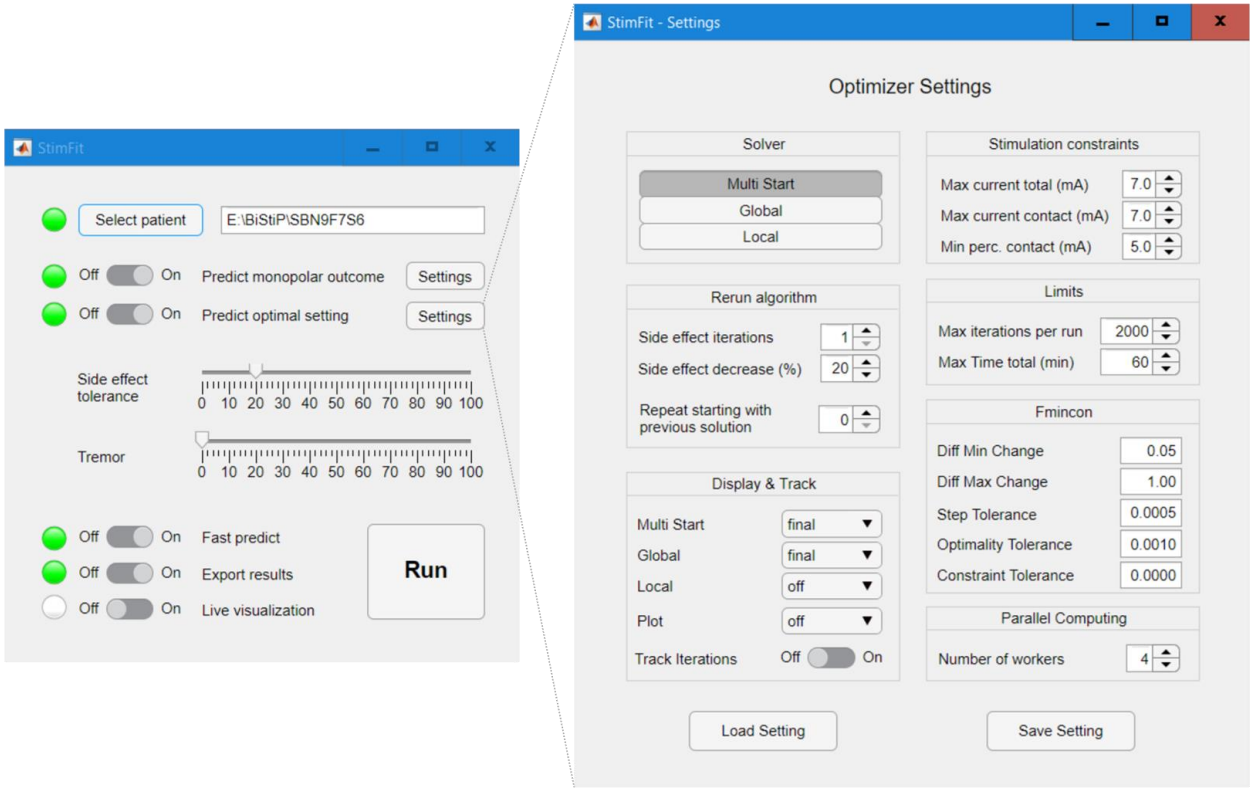

Figure 6: Graphical user interface of StimFit. StimFit was embedded in a MATLAB-based graphical user interface. Left: After reconstruction of DBS electrodes the patient folder (or multiple patients) can be selected. Side-effects and weight of tremor can be adjusted. Right: Different optimizer settings can be selected. The figure shows the default settings used in dissertation study II. Figure from Roediger et al. 2022

2.2.7 Retrospective application

StimFit was applied on all 19 test cohort patients. Maximum side-effect probabilities were set to 20 %. Tremor was excluded from the predictions (slider set to 0 %) forcing the model to find stimulation parameters which would maximize akinetic-rigid symptoms exclusively. Electrodes were reconstructed using Lead-DBS and E-field templates were obtained according to the procedure described in sections 2.2.1 and 2.2.2. A monopolar review was simulated to identify optimal starting points for the multi-start optimizer. Outcome of monopolar stimulation from 0.2 mA to 5 mA was predicted at each contact and stimulation amplitudes with best motor improvements were identified considering the predefined side-effect constraint. These solutions were then used as starting points for the multi-start optimizer. Optimizer settings are shown in **Figure 6**.

2.2.8 Prospective validation (Dissertation study II)

Up to this point we developed and trained a model *(StimFit)* capable of suggesting optimal stimulation parameters in PD patients treated with STN-DBS. While retrospective analyses suggested that model predictions would correspond to good motor symptom control, prospective validation was required to draw confident conclusions about the therapeutic outcome of *StimFit* stimulation parameters. We therefore designed a double-blind 2 x 2 cross-over non-inferiority trial in which standard of care (SoC) as well as *StimFit* stimulation parameters were applied in a randomized order in 35 PD patients treated with STN-DBS. The study protocol is described in detail in **figure 7**. In short, motor scores under *StimFit*, SoC and OFF stimulation conditions were evaluated according to the MDS-UPDRS-III after 45-minutes wash-in/wash-out periods. Additionally, patients were asked to

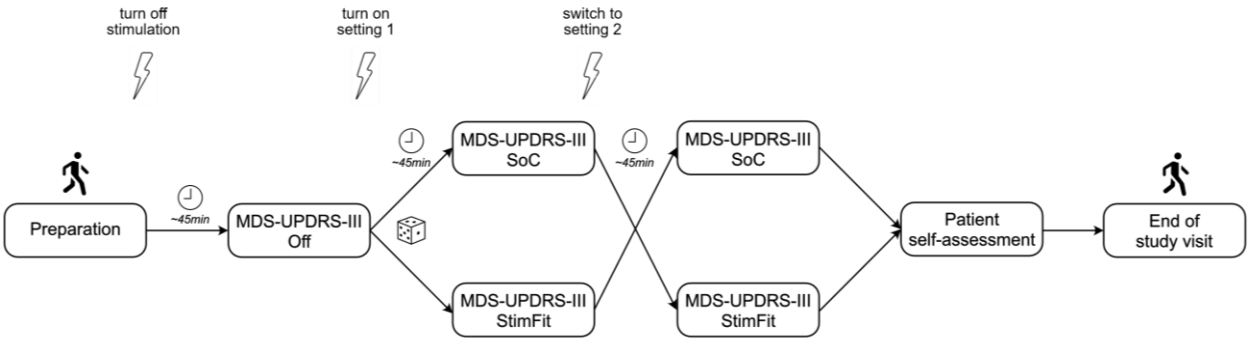

Figure 7: Cross-over design. Patients were invited for study participation after overnight withdrawal of dopaminergic medication. Motor impairment was evaluated in Off-stimulation condition after a 45-minute wash-out period. Standard of Care (SoC) and StimFit stimulation settings were then applied in a double-blind randomized manner (1:1). Again, motor scores were evaluated after a wash-in period of 45 minutes. Finally, patients were asked to self-assess both stimulation conditions and to guess the order of the randomization sequence. Figure from Roediger et al. 2022

subjectively rate the overall effects of both stimulation conditions on a visual analogue scale (VAS) from 0 = “very unsatisfactory” to 100 = “very satisfactory” and to guess the correct order of both conditions.

2.2.8.1 Endpoints and statistical analysis

The primary aim of this study was to establish non-inferiority of *StimFit* stimulation in respect to SoC treatment regarding overall motor symptom control (MDS-UPDRS-III). According to Schrag et al. a non-inferiority margin of five points was defined as clinically significant.[74] A power analysis was conducted based on the cohort described in section 2.1.2 using a one-sided t-test resulting in a required n of 35.

Secondary analyses aimed at evaluating potential differences in stimulation response of specific motor symptoms. We therefore compared differences in MDS-UPDRS-III subscores of akinetic-rigid, tremor and axial items. Further, patients’ VAS self-ratings and estimated battery drain (according to Zhang et al.[75]) under *StimFit* and SoC stimulation were analyzed using Wilcoxon signed rank tests. A two-sided binomial test was applied to assess whether patients could guess the correct sequence of both stimulation conditions above chance level. Significance levels were set to an alpha of 0.05. No adjustments for multiple comparisons were made.

3 Results

Within the scope of the two publications included in this dissertation we developed and validated a data-driven algorithm which could suggest optimal stimulation parameters in PD patients treated with STN-DBS based on reconstructed electrode locations. Following steps were conducted: First, a voxel-segment based ensemble model was developed and trained to predict stimulation outcome (motor improvement as well as side-effect probabilities) based on simulations of the electric field generated by a stimulation setting in the vicinity of the electrode. Next, model predictions were retrospectively validated within the training cohort using cross-validation and tested on an independent dataset. Further, the model was anatomically validated, by comparing optimal stimulation locations (sweet-spots) to literature findings. The predictive model was then embedded in a non-linear optimization algorithm to identify optimal stimulation settings in out-of-sample patients in a time-efficient manner **(Figure 5).** The algorithm (*StimFit*) was implemented in a GUI for a clear and streamlined use **(Figure 6)**. Finally, a randomized cross-over non-inferiority trial was conducted (Dissertation study II) to prospectively assess the effects of DBS settings suggested by StimFit in comparison with those obtained by standard clinical optimization strategies (SoC).

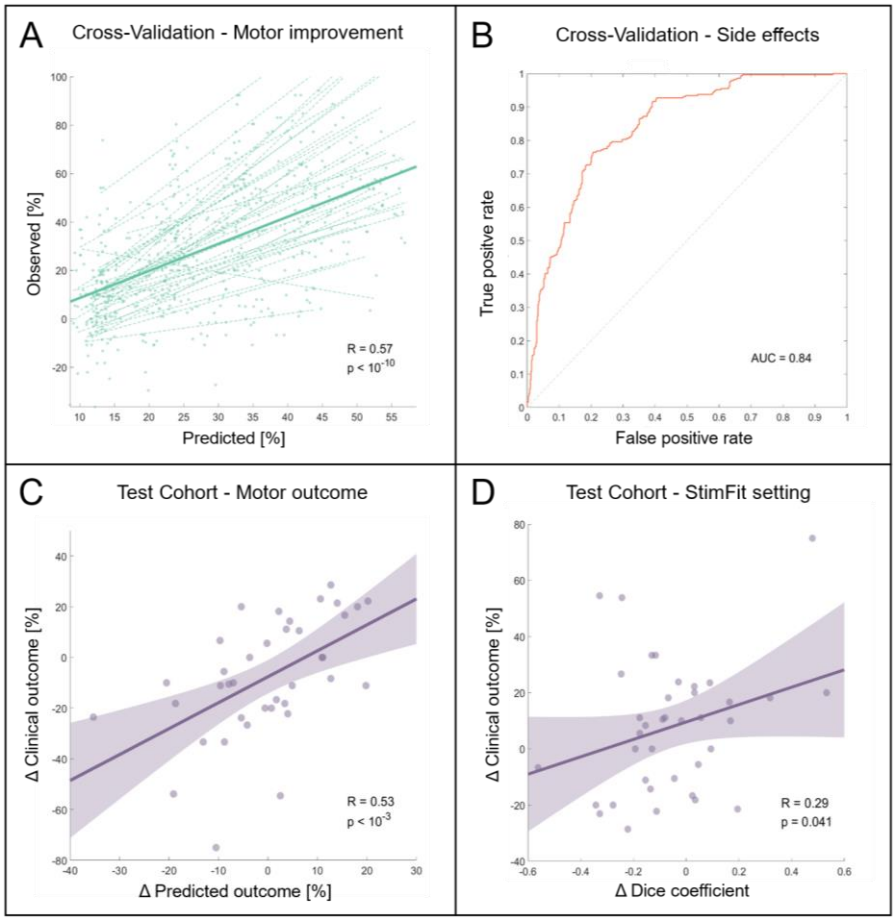

Figure 8: Quantitative retrospective validation. The predictive model (vector field model) was retrospectively validated within the training cohort (cross-validation, panel A and B) and on an independent test dataset (C). Optimizer solutions (StimFit settings) were compared to clinical settings using VTA dice coefficients. Results indicated that clinical settings which showed greater similarities to StimFit settings were associated with superior clinical outcome. Figure adapted from Roediger et al. 2021

3.1 Quantitative retrospective validation (Dissertation Study I)

Predicted motor improvements were correlated to observed improvements within the training cohort (R = 0.57, p < 0.001, **Figure 8A**) as well as in the test cohort (R = 0.53, p < 0.001, **Figure 8B**). Predicted side-effect probabilities resulted in an AUC of 0.84 when compared to observed side-effects **(Figure 8C)**.

3.2 Anatomical validation (Dissertation Study I)

To identify stimulation locations which would lead to optimal motor improvement as well as regions with increased probabilities of eliciting stimulation-induced side-effects 2 mA cathodal stimulations were simulated at 125,000 locations in MNI space and predicted outcome was mapped onto the BigBrain atlas **(Figure 9).**[76] Maximum motor improvement (26 %) was estimated at MNI coordinate x = 13.5, y = -14.0, z = -3.6mm. Increased side-effect probabilities mapped to regions of the ventral STN, substantia nigra pars reticulata and internal capsule compared to lower side-effect probabilities in the dorsal STN, zona incerta and ventral thalamic regions.

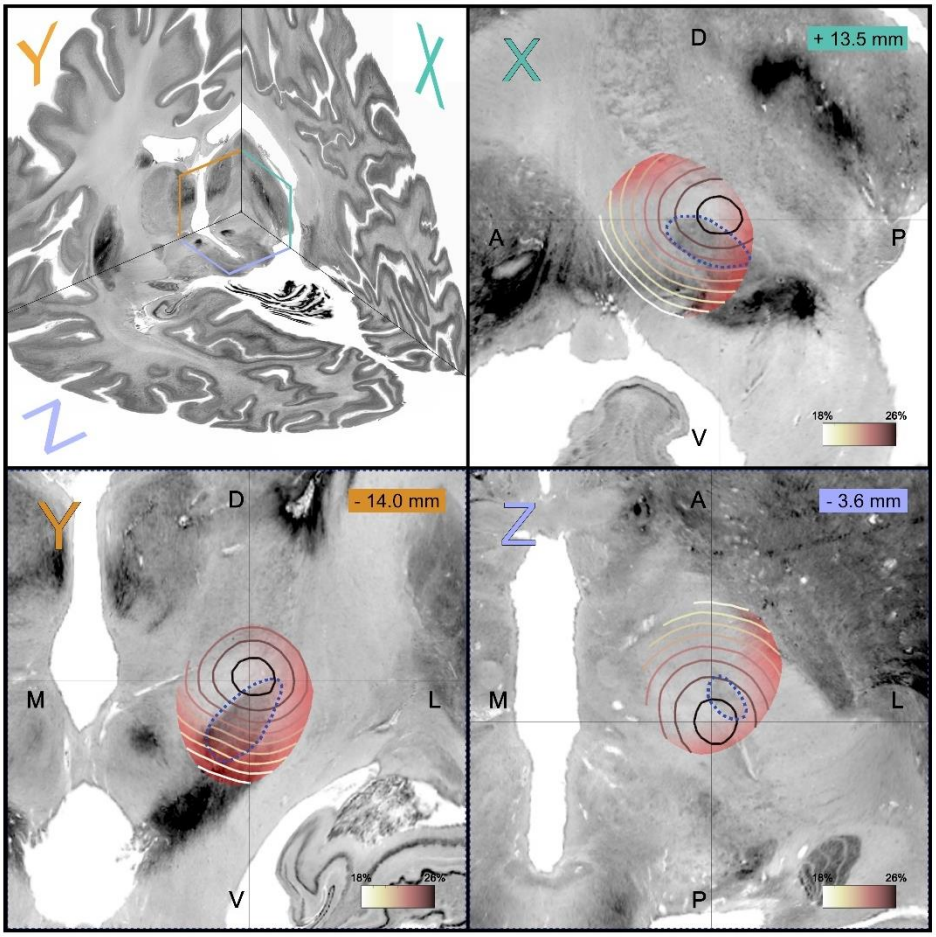

Figure 9: Anatomical validation. Outcome predictions of the vector field model were mapped in respect to the BigBrain atlas. In line with previous literature results, optimal stimulation sites were identified at the dorsolateral region of the STN and its surroundings (black circle). Stimulation sites which were located within the internal capsule and ventral STN were associated with increased side-effect probabilities (red shades). Figure from Roediger et al. 2021

3.3 Retrospective *StimFit* test results (Dissertation Study I)

StimFit was retrospectively tested using electrode locations of 19 patients from the test cohort (section 2.1.2). The software converged to a final solution for both hemispheres in 3005 s ± 269 s including simulations of monopolar reviews (392 s ± 24 s). Overlap between clinical stimulation settings and StimFit suggestions was estimated using Dice-coefficients between resulting VTAs. Large dice coefficients indicate high agreement between both settings and were associated with better clinical improvement (R = 0.29, p = 0.041, **Figure 8D**).

3.4 Prospective validation (Dissertation Study II)

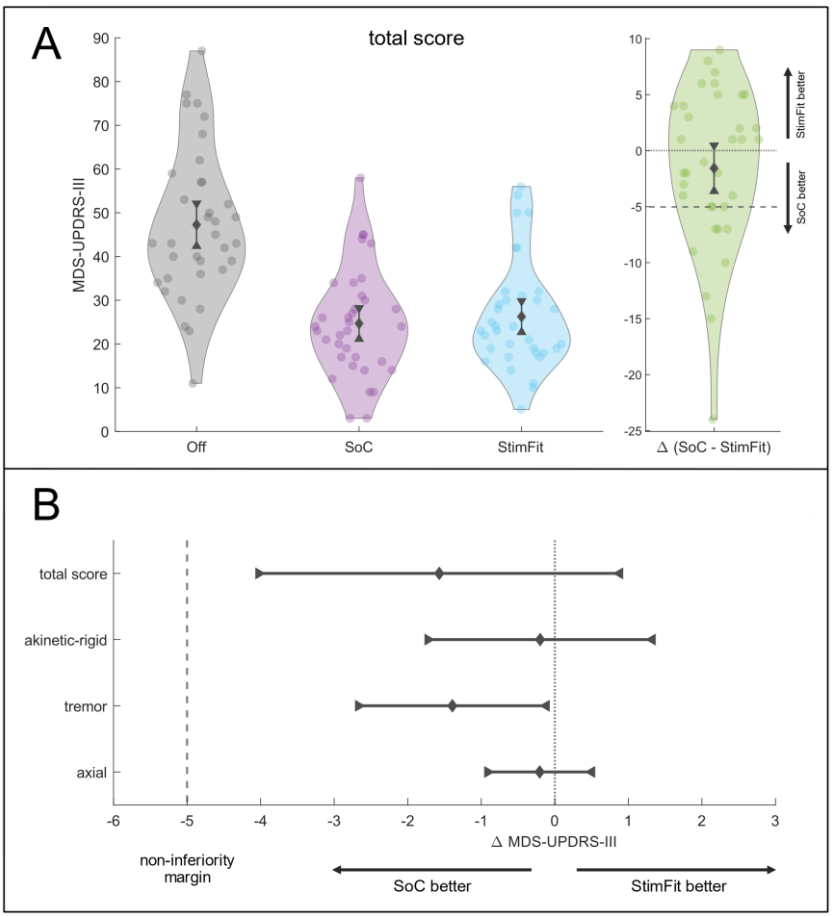

Figure 10: Motor improvement under StimFit and SoC stimulation. Panel A showing the motor scores under Off-, SoC and StimFit stimulation conditions. The primary endpoint (absolute difference between StimFit and SoC stimulation) is shown in green. Mean + 95% confidence intervals are shown in each violin plot. Panel B shows the mean and 95% confidence intervals of the total MDS-UPDRS-III scores along with the symptom-specific sub-scores. Non-inferiority is established since the margin is below the lower 95% confidence interval. Figure from Roediger et al 2022

35 PD patients implanted with directional DBS electrodes at Charité - Universitätsmedizin were recruited for study participation between Oct 2020 and Oct 2021 (section 2.1.3). All study visits were conducted within one day according to the protocol and all patients were included in the primary endpoint analysis.

3.4.1 Primary endpoint

Off-stimulation baseline of MDS-UPDRS-III scores was 47.3 ± 17.1. Motor scores improved to 24.7 ± 12.4 (48 %) under SoC and to 26.3 ± 12.4 (43 %) under *StimFit* stimulation (**Figure 10A**), resulting in a statisti-

cally non-significant advantage of -1.6 ± 7.1 (95% CI: [-4.0, 0.9]) points of SoC stimulation (p_{sup} = 0.20, n = 35). A one-sided t-test was applied showing that this difference was significantly greater than the pre-defined non-inferiority margin of -5 points (p_{noninf} = 0.004), thus establishing non-inferiority of *StimFit* stimulation compared to SoC.

3.4.2 Secondary endpoints

Symptom-specific MDS-UPDRS-III sub-scores **(Figure 10B)** showed no statistically significant differences between both stimulation conditions for akinetic-rigid (-0.2 ± 4.4 (95% CI: [-1.7, 1.3], p = 0.98, n = 35)) and axial symptoms (-0.2 ± 2.0 (95% CI: [-0.9, 0.5], p = 0.67, n = 34)). Tremor suppression was significantly better under SoC stimulation (-1.4 ± 3.3, (95% CI: [-2.7, -0.1], p = 0.046, n= 28)).

Patients' self-assessments (VAS from 0 = "very unsatisfactory" to 100 = "very satisfactory") favored SoC (74 ± 19 points) compared to StimFit (55 ± 24 points) with a mean difference of 19 ± 28, 95% CI: [9, 29], p < 0·001, n = 34, **Figure 11**). 56% of all patients correctly identified the randomization sequence, which was not significantly above chance level (p = 0.50), thus underscoring that patients remained blinded throughout the assessments.

Stimulation-induced side-effects were observed during initial programming of *StimFit* settings in six patients (two muscle contractions, two dysarthria, two vertigo). According to the protocol stimulation amplitudes were reduced in those cases until side-effects disappeared (mean reduction 0.41 ± 0.16 mA ranging from 0.3 to 0.7 mA). Three patients showed delayed onset dyskinesias after 45 minutes wash-in under *StimFit*, two of which were rated as severe. Mild dyskinesias were also observed under SoC stimulation in two cases. Energy consumption of SoC settings was estimated to be 57 ± 29 µA in compared to 50 ± 21 µA for *StimFit* (p = 0.5, n = 32). Additional demographic and treatment related information of individual patients is provided in the original publication.

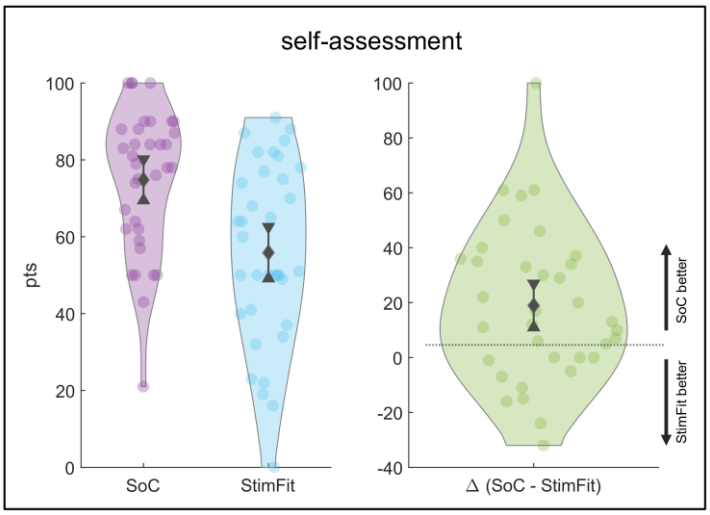

Figure 11: Patient ratings of StimFit and SoC stimulation. Patients were asked to self-assess StimFit and SoC stimulation settings on a visual analogue scale from 0 to 100. Mean and 95 % confidence intervals are shown in each plot. Figure from Roediger et al. 2022

4. Discussion

4.1 Summary of results

The work presented in the scope of this dissertation contains several methodological novelties and provides strong evidence that data-driven models could assist DBS programming based on routinely acquired neuroimaging data. In summary, we developed a predictive model, trained on a large high-quality dataset (n = 612) to derive stimulation outcome of STN-DBS in PD patients (n = 31) on a symptom-specific level. Model predictions were based on electric field simulations, and crucially considered not only the magnitudes but also directionalities of voltage gradients in the vicinity of the electrode. A thorough retrospective validation was conducted in three steps. First, k-fold cross-validation was applied within the training cohort to obtain predictions of motor improvement and side-effect probabilities. Predicted outcome was compared to empirically observed outcome showing strong correlations between predicted and observed motor response (R = 0.57) and classification performance for stimulation induced side-effects (AUC = 0.83). Second, the model was applied on out-of-sample data (n = 19) showing similar performance for motor outcome predictions (R = 0.53). Finally, we simulated DBS at 125,000 anatomical locations in MNI space, mapping predicted outcome to identify regions with optimal motor response or increased probabilities of stimulation-induced side-effects. The “sweet-spots” and regions of avoidance identified this way lined up well with literature results.[24, 30, 39, 40] In the next step the trained and validated model was used to identify optimal stimulation settings in out-of-sample patients based on electrode location. This was done by iteratively simulating varying stimulation settings, obtaining predicted motor improvements and side-effect probabilities in each iteration. In order to converge to an optimal solution in a time-efficient manner, a multi-start gradient descent optimization algorithm was applied. The algorithm (*StimFit*) could now automatically suggest optimal stimulation parameters within ~50 minutes of computation time after electrode reconstructions were provided. *StimFit* is the first software which can automatically suggest optimal multi-contact stimulation settings for DBS. It was embedded in a graphical user interface (**Figure 6**) and made publicly available under https://github.com/JRoediger/StimFit. The second dissertation study aimed at prospectively comparing the imaging-derived settings suggested by *StimFit* to standard of care (SoC) treatment in a cross over, non-inferiority trial. This

study represents the first randomized controlled trial assessing an automated DBS programming algorithm. 35 PD patients were recruited for study participation according to a previously conducted sample size calculation and all patients were included in the final analysis. We found that both *StimFit* and SoC stimulation settings resulted in significant motor improvement compared to OFF-stimulation baseline (43 and 48%). Importantly, no statistically significant difference was found between both stimulation conditions and non-inferiority of *StimFit* stimulation was established.

4.2 Research in context

4.2.1 Predictive modelling based on electric field properties

Large, randomized trials have reported average effects of subthalamic stimulation on motor symptom control in PD patients ranging from 25 to 49 %.[7] However, between individual patients DBS outcome is highly variable. Recent studies were able to explain between 14 to 37 % of outcome variance by electrode placement and stimulation parameters.[24, 26, 30, 77, 78] The performance of these image-based predictive models is highly dependent on the underlying sample characteristics and processing pipelines.[30, 62] Most studies have strongly relied on bottom-up VTA models, which are – from a theoretical standpoint – not ideal to maximize explained outcome variance, as argued in section 1.4.1. One study has applied an E-field based approach to predict STN-DBS outcome and indicated a slight advantage over approaches that build upon binary VTA models.[30] The model which was developed and trained in the first dissertation study has – for the first time – integrated directionalities of E-field gradients in addition to vector magnitudes. This has resulted in an overall R^2 of predicted motor improvement of 32 % within the training cohort and 28 % in an independent test cohort, highlighting that alternatives to VTA-based approaches can perform well and should receive greater attention by the field.

4.2.2 Anatomical implications

Mapping predicted outcome of our trained model in MNI space showed that the optimal location for motor symptom control was situated at the dorsolateral border of the STN.

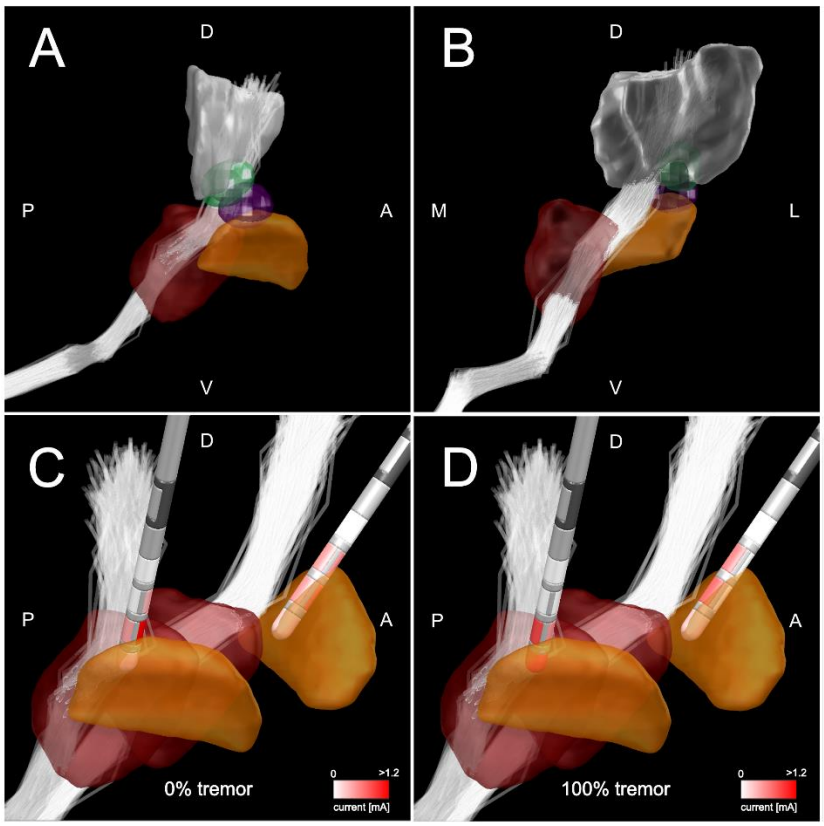

Figure 12: Symptom-specific sweet-spots and stimulation settings. Panels A and B showing the sweet-spots for bradykinesia (purple) and tremor (green) covering the dorsolateral STN (orange) and inferior part of the ventral intermediate part of the thalamus (VIM shown in grey), respectively. The dentato-rubro-thalamic tract, which is considered the target structure, for tremor suppression across diseases is shown in white. Panels C and D show different solutions of StimFit in respect to the target symptom (bradykinesia in panel C and tremor in panel D). Figure from Roediger et al. 2021.

This part of the STN is considered the sensorimotor part **(Figure 2)**, which receives cortical afferents primarily from M1 and within this region electrophysiological abnormalities are most frequently observed in PD patients.[79] The anatomical findings consolidate previously identified "sweet-spots" for STN-DBS.[24, 28, 39, 40, 46, 80] To identify symptom-specific sweet-spots, the analysis was repeated after training the model on tremor or akinetic-rigid items of the UPDRS-III exclusively **(Figure 12A and B)**. The optimal location for suppression of akinesia/rigidity again resided in the sensorimotor STN. The sweet-spot for tremor suppression, however, was located slightly more dorsal and posterior in the zona incerta close to the ventral intermediate nucleus of the thalamus. The peak coordinate is located near the dentato-rubro-thalamic tract. Studies in essential tremor patients with thalamic DBS have shown that the proximity of active DBS contacts to this tract correlates with tremor control.[22, 81-83] Interestingly, this seems to be the case across various diseases, including multiple sclerosis, dystonic tremor as well as PD.[24, 84, 85] The anatomical segregation of symptom-specific sweet-spots in PD has important consequences for automated and image-guided DBS programming, since it impacts the optimal contact selection depending on the symptom profile of the patient **(Figure 12C and D)**.[86]

4.2.3 Mathematical optimization procedures

To identify optimal DBS parameter combinations out of a vast number of combinatorial possibilities, non-linear programming has been applied in previous studies. Conolly et al. have proposed an algorithm which could optimize multiple objectives and suggested that this could be applied using cortical and motor evoked potentials to reduce the DBS parameter space.[87] However, the clinical utility of these electrophysiological biomarkers remains elusive. In a recent pilot study, a constrained optimization algorithm was applied in 15 patients to optimize parameter selection for tremor control based on kinematic feedback.[61] This has resulted in tremor suppression which was comparable to that achieved by clinical optimization. For other parkinsonian symptoms however, algorithm-guided optimization based on kinematic feedback has been less successful.[20] Here, utilizing neuroimaging to identify beneficial DBS settings might be more promising. This has been attempted in several studies, in which biophysical models of axonal activation were applied in mathematical optimization procedures to identify parameter combinations which would maximally engage pre-defined target regions, while avoiding structures that could potentially induce side-effects.[88-91] While these studies were carried out with great methodological detail, they still face the conceptual barriers of mechanistic bottom-up models and therefore seem suboptimal for translational purposes. In the first dissertation study we have, for the first time, embedded a trained and validated data-driven model in a non-linear optimization algorithm to identify optimal DBS parameter combinations in out-of-sample patients. This was done in a two-stage optimization procedure, in which an optimal monopolar solution was identified first (grid-search of 200 settings per electrode), before exploring more complex multi-cathode solutions **(Figure 5)**. In a way, this resembles clinical optimization strategies, in which a monopolar review is conducted first before multipolar settings are considered **(panel “monopolar review”)**. Using optimal monopolar solutions as starting points for the gradient descent optimization algorithm has multiple advantages. First, the starting points are closer to the optimal solution, hence reducing the number of iterations necessary for convergence making the search more time efficient. Along the same lines, starting close to the global optimum reduces the risk of convergence to a local minimum. This was additionally tackled by using multiple starting points (optimal monopolar solution for each contact). Last, the two-step procedure guaranteed that complex multi-cathode solutions were only suggested if their predicted outcome exceeded that of monopolar settings. This optimization procedure could be adapted

for other applications as well, which for example use probabilistic maps or evoked potentials to optimize DBS parameter selection.

4.2.4 Software solutions and prospective applications of image-guided DBS programming

Although the idea to guide DBS programming through computational models and neuroimaging-derived metrics has already been proposed almost two decades ago, commercial software solutions have only recently reached the market and prospective evaluations remain sparse.[92] In their seminal publication Frankemolle et al. applied biophysical models to suggest stimulation settings which would minimize stimulation of nonmotor regions of the STN *in silico.*[93] These settings were prospectively applied in ten patients which then underwent a working memory task. Task performance was superior compared to standard of care stimulation and they concluded that targeting the sensorimotor STN exclusively with the help of image-based models could reduce cognitive decline associated with subthalamic DBS. The software used in this study was bought by Boston Scientific and turned into a commercially available product.[94] The commercial release has prompted prospective studies which emphasized the advantage of software-assisted programming in regard to programming time.[32, 95-97] However, in order to achieve satisfactory therapeutic benefit DBS parameters needed to be re-adjusted based on behavioral feedback. One factor that might be at play resulting in suboptimal clinical effects of current anatomy-based optimizations strategies might be that they require manual selection of parameters in-silico based on VTA-overlap with vaguely defined target structures. Iterative manual steps are not only time-consuming but leave room for different solutions based on the anatomical intuition and training of the programmer. *StimFit* represents the first fully automated algorithm to suggest optimal multi-cathode stimulation configurations on a data-driven basis. In our randomized prospective trial *StimFit* settings resulted in non-inferior motor improvement compared to patients' standard of care treatment, with only minimal adjustments of stimulation amplitudes (amplitude reduction between 0.3 and 0.7 mA) in six patients. This suggests that predictive models embedded in mathematical optimization procedures can identify beneficial DBS settings, which could drastically reduce programming time and resources.

4.3 Limitations

4.3.1 StimFit algorithm (Dissertation study I)

The design, training and retrospective validation of *StimFit* is subject to following limitations. First, *StimFit* is a data-driven model and hence the quality of outcome predictions is highly dependent on the underlying training data. The training dataset consisted of monopolar review data, which was acquired under standardized conditions. Advantages of monopolar review data include an increased intra-individual outcome variation, but clinical outcome of DBS settings might partly be influenced by previous settings due to short wash-in periods. However, no systematic bias can be expected, since the sequence of contact evaluations was randomized in each electrode.

Next, according to standard monopolar review procedures **(panel "monopolar review")**, training data was acquired under a fixed pulse-width of 60 µs and a frequency of 130 Hz. Subsequently, the effects of varying pulse-width or frequencies could not be predicted with our model. Along the same lines, the model is restricted to cathodal stimulation settings and cannot derive bipolar configurations.

Third, motor outcome predictions were tested on an independent dataset from a different center, indicating a good generalizability of the model. However, since this test dataset consisted of optimized chronic DBS settings, side-effect predictions could not be tested independently. In line with literature results, mapping of predicted side-effect probabilities showed increased risks for side-effects when stimulating in the substantia nigra and capsula interna. However, the variance of side-effect probabilities within the target region was quite small, ranging only from 8 to 13 % at 2 mA stimulation amplitudes. This could indicate that predicted side-effect probabilities were primarily driven by stimulation amplitudes opposed to anatomical variation, requiring further investigation and potential adaptation of the side-effect models integrated in *StimFit*.

Finally, our prediction model relies on E-field simulations. A simple homogeneous and isotropic tissue conductivity model was chosen for these simulations to avoid tuning of free model parameters resulting from ambiguities in biophysical tissue properties described in the literature.[98] More complex volume conductor models, as well as adaptations of sampling regions and resolution could further improve model performance.

4.3.2 Clinical trial (Dissertation study II)

Limitations regarding the design of our prospective evaluation of *StimFit* include the following. First, this was a single center study conducted at Charité - Universitätsmedizin Berlin. Neuroimaging sequences at our center were optimized to not only allow for precise surgical targeting, but also to increase precision of electrode reconstructions with our in-house developed software Lead-DBS. While the software is widely used throughout the DBS community around the world, we do not know for certain whether different perioperative imaging protocols would impact the precision of electrode reconstructions and subsequently the performance of *StimFit*. Multi-center investigations are required to assess whether alternative imaging sequences, surgical techniques, or patient cohort characteristics would impact model performance.

Next, study visits were conducted within a single day. While this allowed for a head-to-head comparison of motor performance in OFF-medication states, other endpoints which require longer observational periods could not be evaluated. Specifically, disease related quality of life in PD patients needs to be assessed in future studies, evaluating patients' activities of daily living across multiple dimensions, e.g. through the Parkinson's Disease Questionnaire (PDQ-39). This would require a longitudinal study design, in which DBS settings are applied for at least four weeks.

Finally, our study design does not allow to draw conclusions about potential advantages of *StimFit*-assisted programming with regard to programming time, long-term outcome and medication adjustment. For this a randomized controlled trial, in which patients were assigned to standard or *StimFit* assisted programming immediately after surgery would be ideal. We believe that the promising results of this proof-of-principle study along with the urgent need for better streamlined DBS programming, justify a thorough investigation within large longitudinal randomized controlled trials.

4.4 Implications for practice and future research

4.4.1 Implications for postoperative treatment management and accessibility

According to estimations of the World Health Organization over 8.5 million individuals were living with PD in 2019.[99] This number has doubled within the last 25 years and the disease burden will continue to rise over the next decades especially in countries with a low socio-demographic index.[100] Subthalamic DBS is superior to best medical treatment

in advanced PD patients as well as in patients with early motor complications and could help to drastically decrease disease burden.[8, 101, 102] Yet, annually only 12,000 DBS surgeries are performed worldwide.[103] Reasons for underutilization include lack of appropriate referrals and surgical infrastructure but also concerns about postoperative DBS programming, which is perceived as complex and labor intensive.[104, 105] Scientific and industrial efforts should therefore focus on making DBS more cost-effective and to unburden the complexity of postoperative programming. Current software solutions for image-guided programming may provide advantages in programming time but continue to require highly trained and experienced personnel. (Semi-)automated programming strategies could help streamline postoperative management and potentially reduce the number of programming sessions and the expertise necessary to obtain optimal therapeutic benefit.

4.4.2 Future perspective of multimodal data integration

Within recent years characteristics of local field potentials recorded through the DBS contacts at the stimulation sites have extensively been studied. An excessive oscillatory synchronization in the beta frequency band (13-30 Hz) has been observed in PD patients and linked to severity of motor symptoms.[106] Interestingly, this pathological synchronization can be disrupted through therapy (stimulation as well as medication) which correlates with improvements in motor symptoms.[107, 108] Additionally, the successful use of beta power as a biomarker for adaptive DBS strongly suggests its potential use for guided programming.[109, 110] While previously LFP-recordings were only possible through externalization of DBS electrodes in the immediate postoperative interval, novel neurostimulators allow to record in chronically implanted patients with easy access to electrophysiological recordings on the patient programmer tablet.[111] First steps have been taken to integrate electrophysiological and imaging markers demonstrating that the combination of both modalities could outperform unimodal approaches.[19] Additional integration of intraoperatively recorded electrophysiological signals or evoked potentials could further enhance model predictions.[21, 112] Further, guided DBS parameter optimization based on kinematic feedback has previously been proposed. Wearables can be used to identify bradykinetic states as well as tremor severity suggesting that additional integration of kinematic data could further tailor DBS parameter selection, potentially fully automated in a closed-loop design.[61, 113] Finally, integrating demographic and clinical data into predictive models has shown to increase predictive accuracies.[26, 30] For subthalamic DBS in PD

patients, this is particularly relevant for the presence of tremor, which seems to be optimally controlled in a region more posterior and dorsal to the sweet-spot for akinesia and rigidity and would therefore impact optimal contact selection **(Figure 12A and B)**. *StimFit* already allows to adjust parameter optimization with respect to tremor severity **(Figure 6)** and integration of electrophysiological information is planned. However, whether this would indeed further improve outcome of automated or guided DBS programming needs to be addressed in future prospective trials.

4.4.3 The need for more rigorous prospective trials

In recent years, an overwhelming number of studies has mapped various DBS effects (motor symptoms, quality of life, cognitive and autonomic effects, mood, etc.) to local brain regions or networks across various neurological and psychiatric disorders.[46] Despite the translational value of these findings to improve DBS therapy, prospective applications remain sparse. This is especially worrying since commercial software solutions for image-guided programming are increasingly promoted for clinical use. High-quality clinical trials are required to guarantee optimal treatment benefit for the patients and could also contribute back to fundamental research by identifying valid processing pipelines and models. The prospective study conducted within the scope of this dissertation (study II) represents the largest double-blind trial to assess DBS programming based on neuroimaging data. Despite the promising results, further large randomized controlled trials are required to consolidate the findings, address unanswered questions (e.g., impact on quality of life, overall programming time), identify optimal strategies to integrate image-based programming in clinical routine and to improve current software solutions (e.g., multimodal data integration).

5. Conclusions

Within the two studies presented in this dissertation we developed a novel algorithm to suggest beneficial DBS parameters in an automated fashion based on neuroimaging data. The algorithm was tested retrospectively and in a prospective clinical trial yielding promising results, indicating that image-based DBS programming could achieve motor symptom control comparable to standard clinical treatment. Integrating this approach into clinical routine could reduce programming time and resources, but additional longitudinal studies are required to draw final conclusions about the applicability and long-term outcome of automated image-guided programming strategies.

Reference list

1. Benabid AL, Pollak P, Louveau A, Henry S and de Rougemont J. Combined (thalamotomy and stimulation) stereotactic surgery of the VIM thalamic nucleus for bilateral Parkinson disease. *Appl Neurophysiol*. 1987;50:344-6.

2. Benazzouz A, Gross C, Feger J, Boraud T and Bioulac B. Reversal of rigidity and improvement in motor performance by subthalamic high-frequency stimulation in MPTP-treated monkeys. *Eur J Neurosci*. 1993;5:382-9.

3. Bergman H, Wichmann T and DeLong MR. Reversal of experimental parkinsonism by lesions of the subthalamic nucleus. *Science*. 1990;249:1436-8.

4. Pollak P, Benabid AL, Gross C, Gao DM, Laurent A, Benazzouz A, Hoffmann D, Gentil M and Perret J. [Effects of the stimulation of the subthalamic nucleus in Parkinson disease]. *Rev Neurol (Paris)*. 1993;149:175-6.

5. Siegfried J and Lippitz B. Bilateral chronic electrostimulation of ventroposterolateral pallidum: a new therapeutic approach for alleviating all parkinsonian symptoms. *Neurosurgery*. 1994;35:1126-9; discussion 1129-30.

6. Limousin P, Pollak P, Benazzouz A, Hoffmann D, Le Bas JF, Broussolle E, Perret JE and Benabid AL. Effect of parkinsonian signs and symptoms of bilateral subthalamic nucleus stimulation. *Lancet*. 1995;345:91-5.

7. Krack P, Volkmann J, Tinkhauser G and Deuschl G. Deep Brain Stimulation in Movement Disorders: From Experimental Surgery to Evidence-Based Therapy. *Mov Disord*. 2019;34:1795-1810.

8. Schuepbach WM, Rau J, Knudsen K, Volkmann J, Krack P, Timmermann L, Halbig TD, Hesekamp H, Navarro SM, Meier N, Falk D, Mehdorn M, Paschen S, Maarouf M, Barbe MT, Fink GR, Kupsch A, Gruber D, Schneider GH, Seigneuret E, Kistner A, Chaynes P, Ory-Magne F, Brefel Courbon C, Vesper J, Schnitzler A, Wojtecki L, Houeto JL, Bataille B, Maltete D, Damier P, Raoul S, Sixel-Doering F, Hellwig D, Gharabaghi A, Kruger R, Pinsker MO, Amtage F, Regis JM, Witjas T, Thobois S, Mertens P, Kloss M, Hartmann A, Oertel WH, Post B, Speelman H, Agid Y, Schade-Brittinger C, Deuschl G and Group ES. Neurostimulation for Parkinson's disease with early motor complications. *N Engl J Med*. 2013;368:610-22.

9. Lhommee E, Wojtecki L, Czernecki V, Witt K, Maier F, Tonder L, Timmermann L, Halbig TD, Pineau F, Durif F, Witjas T, Pinsker M, Mehdorn M, Sixel-Doring F, Kupsch A, Kruger R, Elben S, Chabardes S, Thobois S, Brefel-Courbon C, Ory-Magne F, Regis JM, Maltete D, Sauvaget A, Rau J, Schnitzler A, Schupbach M, Schade-Brittinger C, Deuschl G, Houeto JL, Krack P and group Es. Behavioural outcomes of subthalamic stimulation and medical therapy versus medical therapy alone for Parkinson's disease with early motor complications (EARLYSTIM trial): secondary analysis of an open-label randomised trial. *Lancet Neurol*. 2018;17:223-231.

10. Pollo C, Kaelin-Lang A, Oertel MF, Stieglitz L, Taub E, Fuhr P, Lozano AM, Raabe A and Schupbach M. Directional deep brain stimulation: an intraoperative double-blind pilot study. *Brain*. 2014;137:2015-26.

11. Dembek TA, Reker P, Visser-Vandewalle V, Wirths J, Treuer H, Klehr M, Roediger J, Dafsari HS, Barbe MT and Timmermann L. Directional DBS increases side-effect thresholds-A prospective, double-blind trial. *Mov Disord*. 2017;32:1380-1388.

12. Schnitzler A, Mir P, Brodsky MA, Verhagen L, Groppa S, Alvarez R, Evans A, Blazquez M, Nagel S, Pilitsis JG, Potter-Nerger M, Tse W, Almeida L, Tomycz N, Jimenez-Shahed J, Libionka W, Carrillo F, Hartmann CJ, Groiss SJ, Glaser M, Defresne F, Karst E, Cheeran B, Vesper J and Investigators PS. Directional Deep Brain Stimulation for Parkinson's Disease: Results of an International Crossover Study With Randomized, Double-Blind Primary Endpoint. *Neuromodulation*. 2022;25:817-828.

13. Anderson DN, Anderson C, Lanka N, Sharma R, Butson CR, Baker BW and Dorval AD. The muDBS: Multiresolution, Directional Deep Brain Stimulation for Improved Targeting of Small Diameter Fibers. *Front Neurosci*. 2019;13:1152.

14. Picillo M, Lozano AM, Kou N, Puppi Munhoz R and Fasano A. Programming Deep Brain Stimulation for Parkinson's Disease: The Toronto Western Hospital Algorithms. *Brain Stimul*. 2016;9:425-437.

15. Volkmann J, Moro E and Pahwa R. Basic algorithms for the programming of deep brain stimulation in Parkinson's disease. *Mov Disord*. 2006;21 Suppl 14:S284-9.

16. Temperli P, Ghika J, Villemure JG, Burkhard PR, Bogousslavsky J and Vingerhoets FJ. How do parkinsonian signs return after discontinuation of subthalamic DBS? *Neurology*. 2003;60:78-81.

17. Dale J, Schmidt SL, Mitchell K, Turner DA and Grill WM. Evoked potentials generated by deep brain stimulation for Parkinson's disease. *Brain Stimul*. 2022;15:1040-1047.

18. Loh A, Gwun D, Chow CT, Boutet A, Tasserie J, Germann J, Santyr B, Elias G, Yamamoto K, Sarica C, Vetkas A, Zemmar A, Madhavan R, Fasano A and Lozano AM. Probing responses to deep brain stimulation with functional magnetic resonance imaging. *Brain Stimul*. 2022;15:683-694.

19. Shah A, Nguyen TK, Peterman K, Khawaldeh S, Debove I, Shah SA, Torrecillos F, Tan H, Pogosyan A, Lachenmayer ML, Michelis J, Brown P, Pollo C, Krack P, Nowacki A and Tinkhauser G. Combining Multimodal Biomarkers to Guide Deep Brain Stimulation Programming in Parkinson Disease. *Neuromodulation*. 2022.

20. Wenzel GR, Roediger J, Brucke C, Marcelino ALA, Gulke E, Potter-Nerger M, Scholtes H, Wynants K, Juarez Paz LM and Kuhn AA. CLOVER-DBS: Algorithm-Guided Deep Brain Stimulation-Programming Based on External Sensor Feedback Evaluated in a Prospective, Randomized, Crossover, Double-Blind, Two-Center Study. *J Parkinsons Dis*. 2021.

21. Xu SS, Sinclair NC, Bulluss KJ, Perera T, Lee WL, McDermott HJ and Thevathasan W. Towards guided and automated programming of subthalamic area stimulation in Parkinson's disease. *Brain Commun*. 2022;4:fcac003.

22. Al-Fatly B, Ewert S, Kubler D, Kroneberg D, Horn A and Kuhn AA. Connectivity profile of thalamic deep brain stimulation to effectively treat essential tremor. *Brain*. 2019;142:3086-3098.

23. Baldermann JC, Melzer C, Zapf A, Kohl S, Timmermann L, Tittgemeyer M, Huys D, Visser-Vandewalle V, Kuhn AA, Horn A and Kuhn J. Connectivity Profile Predictive of Effective Deep Brain Stimulation in Obsessive-Compulsive Disorder. *Biol Psychiatry*. 2019.

24. Dembek TA, Roediger J, Horn A, Reker P, Oehrn C, Dafsari HS, Li N, Kuhn AA, Fink GR, Visser-Vandewalle V, Barbe MT and Timmermann L. Probabilistic sweet spots predict motor outcome for deep brain stimulation in Parkinson disease. *Ann Neurol*. 2019;86:527-538.

25. Ganos C, Al-Fatly B, Fischer JF, Baldermann JC, Hennen C, Visser-Vandewalle V, Neudorfer C, Martino D, Li J, Bouwens T, Ackermanns L, Leentjens AFG, Pyatigorskaya N, Worbe Y, Fox MD, Kuhn AA and Horn A. A neural network for tics: insights from causal brain lesions and deep brain stimulation. *Brain*. 2022.

26. Horn A, Reich M, Vorwerk J, Li N, Wenzel G, Fang Q, Schmitz-Hubsch T, Nickl R, Kupsch A, Volkmann J, Kuhn AA and Fox MD. Connectivity Predicts deep brain stimulation outcome in Parkinson disease. *Ann Neurol*. 2017;82:67-78.

27. Piper RJ, Richardson RM, Worrell G, Carmichael DW, Baldeweg T, Litt B, Denison T and Tisdall MM. Towards network-guided neuromodulation for epilepsy. *Brain*. 2022.

28. Boutet A, Germann J, Gwun D, Loh A, Elias GJB, Neudorfer C, Paff M, Horn A, Kuhn AA, Munhoz RP, Kalia SK, Hodaie M, Kucharczyk W, Fasano A and Lozano AM. Sign-specific stimulation 'hot' and 'cold' spots in Parkinson's disease validated with machine learning. *Brain Commun*. 2021;3:fcab027.

29. Horn A and Kuhn AA. Lead-DBS: a toolbox for deep brain stimulation electrode localizations and visualizations. *Neuroimage*. 2015;107:127-35.

30. Horn A, Li N, Dembek TA, Kappel A, Boulay C, Ewert S, Tietze A, Husch A, Perera T, Neumann WJ, Reisert M, Si H, Oostenveld R, Rorden C, Yeh FC, Fang Q, Herrington TM, Vorwerk J and Kuhn AA. Lead-DBS v2: Towards a comprehensive pipeline for deep brain stimulation imaging. *Neuroimage*. 2019;184:293-316.

31. Noecker AM, Frankemolle-Gilbert AM, Howell B, Petersen MV, Beylergil SB, Shaikh AG and McIntyre CC. StimVision v2: Examples and Applications in Subthalamic Deep Brain Stimulation for Parkinson's Disease. *Neuromodulation*. 2021;24:248-258.

32. Pavese N, Tai YF, Yousif N, Nandi D and Bain PG. Traditional Trial and Error versus Neuroanatomic 3-Dimensional Image Software-Assisted Deep Brain Stimulation Programming in Patients with Parkinson Disease. *World Neurosurg*. 2020;134:e98-e102.

33. Butson CR, Noecker AM, Maks CB and McIntyre CC. StimExplorer: deep brain stimulation parameter selection software system. *Acta Neurochir Suppl*. 2007;97:569-74.

34. McIntyre CC, Grill WM, Sherman DL and Thakor NV. Cellular effects of deep brain stimulation: model-based analysis of activation and inhibition. *J Neurophysiol*. 2004;91:1457-69.

35. Butson CR, Cooper SE, Henderson JM and McIntyre CC. Patient-specific analysis of the volume of tissue activated during deep brain stimulation. *Neuroimage*. 2007;34:661-70.

36. McIntyre CC, Miocinovic S and Butson CR. Computational analysis of deep brain stimulation. *Expert Rev Med Devices*. 2007;4:615-22.

37. Butson CR and McIntyre CC. Current steering to control the volume of tissue activated during deep brain stimulation. *Brain Stimul*. 2008;1:7-15.

38. Astrom M, Diczfalusy E, Martens H and Wardell K. Relationship between neural activation and electric field distribution during deep brain stimulation. *IEEE Trans Biomed Eng*. 2015;62:664-672.

39. Caire F, Ranoux D, Guehl D, Burbaud P and Cuny E. A systematic review of studies on anatomical position of electrode contacts used for chronic subthalamic stimulation in Parkinson's disease. *Acta Neurochir (Wien)*. 2013;155:1647-54; discussion 1654.

40. Bot M, Schuurman PR, Odekerken VJJ, Verhagen R, Contarino FM, De Bie RMA and van den Munckhof P. Deep brain stimulation for Parkinson's disease: defining the optimal location within the subthalamic nucleus. *J Neurol Neurosurg Psychiatry*. 2018;89:493-498.

41. Ashby P, Kim YJ, Kumar R, Lang AE and Lozano AM. Neurophysiological effects of stimulation through electrodes in the human subthalamic nucleus. *Brain*. 1999;122 (Pt 10):1919-31.

42. Butson CR and McIntyre CC. Role of electrode design on the volume of tissue activated during deep brain stimulation. *J Neural Eng*. 2006;3:1-8.

43. Butson CR and McIntyre CC. Tissue and electrode capacitance reduce neural activation volumes during deep brain stimulation. *Clin Neurophysiol*. 2005;116:2490-500.

44. Hines ML and Carnevale NT. NEURON: a tool for neuroscientists. *Neuroscientist*. 2001;7:123-35.

45. Reich MM, Horn A, Lange F, Roothans J, Paschen S, Runge J, Wodarg F, Pozzi NG, Witt K, Nickl RC, Soussand L, Ewert S, Maltese V, Wittstock M, Schneider GH, Coenen V, Mahlknecht P, Poewe W, Eisner W, Helmers AK, Matthies C, Sturm V, Isaias IU, Krauss JK, Kuhn AA, Deuschl G and Volkmann J. Probabilistic mapping of the antidystonic effect of pallidal neurostimulation: a multicentre imaging study. *Brain*. 2019.

46. Horn A. The impact of modern-day neuroimaging on the field of deep brain stimulation. *Curr Opin Neurol*. 2019;32:511-520.

47. Horn A and Fox MD. Opportunities of connectomic neuromodulation. *Neuroimage*. 2020;221:117180.

48. Fox MD, Buckner RL, Liu H, Chakravarty MM, Lozano AM and Pascual-Leone A. Resting-state networks link invasive and noninvasive brain stimulation across diverse psychiatric and neurological diseases. *Proc Natl Acad Sci U S A*. 2014;111:E4367-75.

49. Lehto LJ, Slopsema JP, Johnson MD, Shatillo A, Teplitzky BA, Utecht L, Adriany G, Mangia S, Sierra A, Low WC, Grohn O and Michaeli S. Orientation selective deep brain stimulation. *J Neural Eng*. 2017;14:016016.

50. Anderson DN, Duffley G, Vorwerk J, Dorval AD and Butson CR. Anodic stimulation misunderstood: preferential activation of fiber orientations with anodic waveforms in deep brain stimulation. *J Neural Eng*. 2019;16:016026.

51. Frankemolle-Gilbert AM, Howell B, Bower KL, Veltink PH, Heida T and McIntyre CC. Comparison of methodologies for modeling directional deep brain stimulation electrodes. *PLoS One*. 2021;16:e0260162.

52. Grasso M, Albantakis L, Lang JP and Tononi G. Causal reductionism and causal structures. *Nat Neurosci*. 2021;24:1348-1355.

53. Krakauer JW, Ghazanfar AA, Gomez-Marin A, MacIver MA and Poeppel D. Neuroscience Needs Behavior: Correcting a Reductionist Bias. *Neuron*. 2017;93:480-490.

54. Anderson PW. More Is Different. *Science*. 1972;177:393-396.

55. Das S, Trutoiu L, Murai A, Alcindor D, Oh M, De la Torre F and Hodgins J. Quantitative measurement of motor symptoms in Parkinson's disease: a study with full-body motion capture data. *Annu Int Conf IEEE Eng Med Biol Soc*. 2011;2011:6789-92.

56. Khosravi M, Atashzar SF, Gilmore G, Jog MS and Patel RV. Intraoperative Localization of STN During DBS Surgery Using a Data-Driven Model. *IEEE J Transl Eng Health Med*. 2020;8:2500309.

57. Farrokhi F, Buchlak QD, Sikora M, Esmaili N, Marsans M, McLeod P, Mark J, Cox E, Bennett C and Carlson J. Investigating Risk Factors and Predicting Complications in Deep Brain Stimulation Surgery with Machine Learning Algorithms. *World Neurosurg*. 2020;134:e325-e338.

58. Habets JGV, Heijmans M, Kuijf ML, Janssen MLF, Temel Y and Kubben PL. An update on adaptive deep brain stimulation in Parkinson's disease. *Mov Disord*. 2018;33:1834-1843.

59. Merk T, Peterson V, Lipski WJ, Blankertz B, Turner RS, Li N, Horn A, Richardson RM and Neumann WJ. Electrocorticography is superior to subthalamic local field potentials for movement decoding in Parkinson's disease. *Elife*. 2022;11.

60. Neumann WJ, Turner RS, Blankertz B, Mitchell T, Kuhn AA and Richardson RM. Toward Electrophysiology-Based Intelligent Adaptive Deep Brain Stimulation for Movement Disorders. *Neurotherapeutics*. 2019;16:105-118.

61. Sarikhani P, Ferleger B, Mitchell K, Ostrem J, Herron J, Mahmoudi B and Miocinovic S. Automated deep brain stimulation programming with safety constraints for tremor suppression in patients with Parkinson's disease and essential tremor. *J Neural Eng*. 2022;19.

62. Dembek TA, Baldermann JC, Petry-Schmelzer JN, Jergas H, Treuer H, Visser-Vandewalle V, Dafsari HS and Barbe MT. Sweetspot Mapping in Deep Brain Stimulation: Strengths and Limitations of Current Approaches. *Neuromodulation*. 2022;25:877-887.

63. Roediger J, Dembek TA, Wenzel G, Butenko K, Kuhn AA and Horn A. StimFit-A Data-Driven Algorithm for Automated Deep Brain Stimulation Programming. *Mov Disord*. 2021.

64. Roediger J, Dembek TA, Achtzehn J, Busch JL, Kramer AP, Faust K, Schneider GH, Krause P, Horn A and Kuhn AA. Automated deep brain stimulation programming based on electrode location: a randomised, crossover trial using a data-driven algorithm. *Lancet Digit Health*. 2022.

65. Acton PD and Friston KJ. Statistical parametric mapping in functional neuroimaging: beyond PET and fMRI activation studies. *Eur J Nucl Med*. 1998;25:663-7.

66. Avants BB, Epstein CL, Grossman M and Gee JC. Symmetric diffeomorphic image registration with cross-correlation: evaluating automated labeling of elderly and neurodegenerative brain. *Med Image Anal*. 2008;12:26-41.

67. Fonov V, Evans AC, Botteron K, Almli CR, McKinstry RC, Collins DL and Brain Development Cooperative G. Unbiased average age-appropriate atlases for pediatric studies. *Neuroimage*. 2011;54:313-27.

68. Schonecker T, Kupsch A, Kuhn AA, Schneider GH and Hoffmann KT. Automated optimization of subcortical cerebral MR imaging-atlas coregistration for improved postoperative electrode localization in deep brain stimulation. *AJNR Am J Neuroradiol*. 2009;30:1914-21.

69. Oxenford S, Roediger J, Neudorfer C, Milosevic L, Guttler C, Spindler P, Vajkoczy P, Neumann WJ, Kuhn A and Horn A. Lead-OR: A multimodal platform for deep brain stimulation surgery. *Elife*. 2022;11.

70. Hellerbach A, Dembek TA, Hoevels M, Holz JA, Gierich A, Luyken K, Barbe MT, Wirths J, Visser-Vandewalle V and Treuer H. DiODe: Directional Orientation Detection of Segmented Deep Brain Stimulation Leads: A Sequential Algorithm Based on CT Imaging. *Stereotact Funct Neurosurg*. 2018;96:335-341.

71. Husch A, M VP, Gemmar P, Goncalves J and Hertel F. PaCER - A fully automated method for electrode trajectory and contact reconstruction in deep brain stimulation. *Neuroimage Clin*. 2018;17:80-89.

72. Si H. TetGen, a Delaunay-Based Quality Tetrahedral Mesh Generator. *ACM Transactions on Mathematical Software*. 2015;42:1-36.

73. Baniasadi M, Proverbio D, Goncalves J, Hertel F and Husch A. FastField: An open-source toolbox for efficient approximation of deep brain stimulation electric fields. *Neuroimage*. 2020;223:117330.

74. Schrag A, Sampaio C, Counsell N and Poewe W. Minimal clinically important change on the unified Parkinson's disease rating scale. *Mov Disord*. 2006;21:1200-7.

75. Zhang S, Silburn P, Pouratian N, Cheeran B, Venkatesan L, Kent A and Schnitzler A. Comparing Current Steering Technologies for Directional Deep Brain Stimulation Using a Computational Model That Incorporates Heterogeneous Tissue Properties. *Neuromodulation*. 2020;23:469-477.

76. Amunts K, Lepage C, Borgeat L, Mohlberg H, Dickscheid T, Rousseau ME, Bludau S, Bazin PL, Lewis LB, Oros-Peusquens AM, Shah NJ, Lippert T, Zilles K and Evans AC. BigBrain: an ultrahigh-resolution 3D human brain model. *Science*. 2013;340:1472-5.

77. Elias GJB, Boutet A, Joel SE, Germann J, Gwun D, Neudorfer C, Gramer RM, Algarni M, Paramanandam V, Prasad S, Beyn ME, Horn A, Madhavan R, Ranjan M, Lozano CS, Kuhn AA, Ashe J, Kucharczyk W, Munhoz RP, Giacobbe P, Kennedy SH, Woodside DB, Kalia SK, Fasano A, Hodaie M and Lozano AM. Probabilistic Mapping of Deep Brain Stimulation: Insights from 15 Years of Therapy. *Ann Neurol*. 2021;89:426-443.

78. Todt I, Al-Fatly B, Granert O, Kuhn AA, Krack P, Rau J, Timmermann L, Schnitzler A, Paschen S, Helmers AK, Hartmann A, Bardinet E, Schuepbach M, Barbe MT, Dembek TA, Fraix V, Kubler D, Brefel-Courbon C, Gharabaghi A, Wojtecki L, Pinsker MO, Thobois S, Damier P, Witjas T, Houeto JL, Schade-Brittinger C, Vidailhet M, Horn A and Deuschl G. The Contribution of Subthalamic Nucleus Deep Brain Stimulation to the Improvement in Motor Functions and Quality of Life. *Mov Disord*. 2022;37:291-301.

79. Horn A, Neumann WJ, Degen K, Schneider GH and Kuhn AA. Toward an electrophysiological "sweet spot" for deep brain stimulation in the subthalamic nucleus. *Hum Brain Mapp*. 2017.

80. Akram H, Sotiropoulos SN, Jbabdi S, Georgiev D, Mahlknecht P, Hyam J, Foltynie T, Limousin P, De Vita E, Jahanshahi M, Hariz M, Ashburner J, Behrens T and Zrinzo L. Subthalamic deep brain stimulation sweet spots and hyperdirect cortical connectivity in Parkinson's disease. *Neuroimage*. 2017;158:332-345.

81. Dembek TA, Barbe MT, Astrom M, Hoevels M, Visser-Vandewalle V, Fink GR and Timmermann L. Probabilistic mapping of deep brain stimulation effects in essential tremor. *Neuroimage Clin*. 2017;13:164-173.

82. Nowacki A, Barlatey S, Al-Fatly B, Dembek T, Bot M, Green AL, Kubler D, Lachenmayer ML, Debove I, Segura-Amil A, Horn A, Visser-Vandewalle V, Schuurman R, Barbe M, Aziz TZ, Kuhn AA, Nguyen TAK and Pollo C. Probabilistic Mapping Reveals Optimal Stimulation Site in Essential Tremor. *Ann Neurol*. 2022;91:602-612.

83. Petry-Schmelzer JN, Dembek TA, Steffen JK, Jergas H, Dafsari HS, Fink GR, Visser-Vandewalle V and Barbe MT. Selecting the Most Effective DBS Contact in Essential Tremor Patients Based on Individual Tractography. *Brain Sci*. 2020;10.

84. Abdulbaki A, Kaufmann J, Galazky I, Buentjen L and Voges J. Neuromodulation of the subthalamic nucleus in Parkinson's disease: the effect of fiber tract stimulation on tremor control. *Acta Neurochir (Wien)*. 2021;163:185-195.

85. Coenen VA, Sajonz B, Prokop T, Reisert M, Piroth T, Urbach H, Jenkner C and Reinacher PC. The dentato-rubro-thalamic tract as the potential common deep brain stimulation target for tremor of various origin: an observational case series. *Acta Neurochir (Wien)*. 2020;162:1053-1066.

86. Hollunder B, Rajamani N, Siddiqi SH, Finke C, Kuhn AA, Mayberg HS, Fox MD, Neudorfer C and Horn A. Toward personalized medicine in connectomic deep brain stimulation. *Prog Neurobiol*. 2022;210:102211.

87. Connolly MJ, Cole ER, Isbaine F, de Hemptinne C, Starr PA, Willie JT, Gross RE and Miocinovic S. Multi-objective data-driven optimization for improving deep brain stimulation in Parkinson's disease. *J Neural Eng*. 2021;18.

88. Anderson DN, Osting B, Vorwerk J, Dorval AD and Butson CR. Optimized programming algorithm for cylindrical and directional deep brain stimulation electrodes. *J Neural Eng*. 2018;15:026005.

89. Pena E, Zhang S, Patriat R, Aman JE, Vitek JL, Harel N and Johnson MD. Multi-objective particle swarm optimization for postoperative deep brain stimulation targeting of subthalamic nucleus pathways. *J Neural Eng*. 2018;15:066020.

90. Vorwerk J, McCann D, Kruger J and Butson CR. Interactive computation and visualization of deep brain stimulation effects using Duality. *Comput Methods Biomech Biomed Eng Imaging Vis*. 2020;8:3-14.

91. Malekmohammadi M, Mustakos R, Sheth S, Pouratian N, McIntyre CC, Bijanki KR, Tsolaki E, Chiu K, Robinson ME, Adkinson JA, Oswalt D and Carcieri S. Automated optimization of deep brain stimulation parameters for modulating neuroimaging-based targets. *J Neural Eng*. 2022;19.

92. McIntyre CC, Mori S, Sherman DL, Thakor NV and Vitek JL. Electric field and stimulating influence generated by deep brain stimulation of the subthalamic nucleus. *Clin Neurophysiol*. 2004;115:589-95.

93. Frankemolle AM, Wu J, Noecker AM, Voelcker-Rehage C, Ho JC, Vitek JL, McIntyre CC and Alberts JL. Reversing cognitive-motor impairments in Parkinson's disease patients using a computational modelling approach to deep brain stimulation programming. *Brain*. 2010;133:746-61.

94. Miocinovic S, Noecker AM, Maks CB, Butson CR and McIntyre CC. Cicerone: stereotactic neurophysiological recording and deep brain stimulation electrode placement software system. *Acta Neurochir Suppl*. 2007;97:561-7.

95. Pourfar MH, Mogilner AY, Farris S, Giroux M, Gillego M, Zhao Y, Blum D, Bokil H and Pierre MC. Model-Based Deep Brain Stimulation Programming for Parkinson's Disease: The GUIDE Pilot Study. *Stereotact Funct Neurosurg*. 2015;93:231-9.

96. Waldthaler J, Bopp M, Kuhn N, Bacara B, Keuler M, Gjorgjevski M, Carl B, Timmermann L, Nimsky C and Pedrosa DJ. Imaging-based programming of subthalamic nucleus deep brain stimulation in Parkinson's disease. *Brain Stimul*. 2021;14:1109-1117.

97. Lange F, Steigerwald F, Malzacher T, Brandt GA, Odorfer TM, Roothans J, Reich MM, Fricke P, Volkmann J, Matthies C and Capetian PD. Reduced Programming Time and Strong Symptom Control Even in Chronic Course Through Imaging-Based DBS Programming. *Front Neurol*. 2021;12:785529.

98. McCann H, Pisano G and Beltrachini L. Variation in Reported Human Head Tissue Electrical Conductivity Values. *Brain Topogr*. 2019;32:825-858.

99. Organization WH. Global Health Estimates 2020: Disease burden by Cause, Age, Sex, by Country and by Region, 2000-2019. 2020.

100. Collaborators GBDPsD. Global, regional, and national burden of Parkinson's disease, 1990-2016: a systematic analysis for the Global Burden of Disease Study 2016. *Lancet Neurol*. 2018;17:939-953.

101. Weaver FM, Follett K, Stern M, Hur K, Harris C, Marks WJ, Jr., Rothlind J, Sagher O, Reda D, Moy CS, Pahwa R, Burchiel K, Hogarth P, Lai EC, Duda JE, Holloway K, Samii A, Horn S, Bronstein J, Stoner G, Heemskerk J, Huang GD and Group CSPS. Bilateral deep brain stimulation vs best medical therapy for patients with advanced Parkinson disease: a randomized controlled trial. *JAMA*. 2009;301:63-73.

102. Williams A, Gill S, Varma T, Jenkinson C, Quinn N, Mitchell R, Scott R, Ives N, Rick C, Daniels J, Patel S, Wheatley K and Group PSC. Deep brain stimulation plus best medical therapy versus best medical therapy alone for advanced Parkinson's disease (PD SURG trial): a randomised, open-label trial. *Lancet Neurol*. 2010;9:581-91.

103. Lee DJ, Lozano CS, Dallapiazza RF and Lozano AM. Current and future directions of deep brain stimulation for neurological and psychiatric disorders. *J Neurosurg*. 2019;131:333-342.

104. Shih LC and Tarsy D. Survey of U.S. neurologists' attitudes towards deep brain stimulation for Parkinson's disease. *Neuromodulation*. 2011;14:208-13; discussion 213.

105. Zhang C, Ramirez-Zamora A, Meng F, Lin Z, Lai Y, Li D, Chang J, Morishita T, Inoue T, Fujioka S, Oyama G, Coyne T, Voon V, Doshi PK, Wu Y, Liu J, Patel B, Almeida L, Wagle Shukla AA, Hu W, Foote K, Zhang J, Sun B and Okun MS. An International Survey of Deep Brain Stimulation Utilization in Asia and Oceania: The DBS Think Tank East. *Front Hum Neurosci*. 2020;14:162.

106. Kuhn AA, Tsui A, Aziz T, Ray N, Brucke C, Kupsch A, Schneider GH and Brown P. Pathological synchronisation in the subthalamic nucleus of patients with Parkinson's disease relates to both bradykinesia and rigidity. *Exp Neurol*. 2009;215:380-7.

107. Kuhn AA, Kupsch A, Schneider GH and Brown P. Reduction in subthalamic 8-35 Hz oscillatory activity correlates with clinical improvement in Parkinson's disease. *Eur J Neurosci*. 2006;23:1956-60.

108. Kuhn AA, Kempf F, Brucke C, Gaynor Doyle L, Martinez-Torres I, Pogosyan A, Trottenberg T, Kupsch A, Schneider GH, Hariz MI, Vandenberghe W, Nuttin B and Brown P. High-frequency stimulation of the subthalamic nucleus suppresses oscillatory beta activity in patients with Parkinson's disease in parallel with improvement in motor performance. *J Neurosci*. 2008;28:6165-73.

109. Tinkhauser G, Pogosyan A, Debove I, Nowacki A, Shah SA, Seidel K, Tan H, Brittain JS, Petermann K, di Biase L, Oertel M, Pollo C, Brown P and Schuepbach M. Directional local field potentials: A tool to optimize deep brain stimulation. *Mov Disord*. 2018;33:159-164.

110. Zaidel A, Spivak A, Grieb B, Bergman H and Israel Z. Subthalamic span of beta oscillations predicts deep brain stimulation efficacy for patients with Parkinson's disease. *Brain*. 2010;133:2007-21.

111. Feldmann LK, Lofredi R, Neumann WJ, Al-Fatly B, Roediger J, Bahners BH, Nikolov P, Denison T, Saryyeva A, Krauss JK, Faust K, Florin E, Schnitzler A, Schneider GH and Kuhn AA. Toward therapeutic electrophysiology: beta-band suppression as a biomarker in chronic local field potential recordings. *NPJ Parkinsons Dis*. 2022;8:44.

112. Howell B, Isbaine F, Willie JT, Opri E, Gross RE, De Hemptinne C, Starr PA, McIntyre CC and Miocinovic S. Image-based biophysical modeling predicts cortical potentials evoked with subthalamic deep brain stimulation. *Brain Stimul*. 2021;14:549-563.

113. Habets JGV, Herff C, Kubben PL, Kuijf ML, Temel Y, Evers LJW, Bloem BR, Starr PA, Gilron R and Little S. Rapid Dynamic Naturalistic Monitoring of Bradykinesia in Parkinson's Disease Using a Wrist-Worn Accelerometer. *Sensors (Basel)*. 2021;21.

Statutory Declaration

“I, Jan Roediger, by personally signing this document in lieu of an oath, hereby affirm that I prepared the submitted dissertation on the topic “Towards automated deep brain stimulation programming” (German Title: “Auf dem Weg zur automatisierten Programmierung der tiefen Hirnstimulation”) independently and without the support of third parties, and that I used no other sources and aids than those stated.
All parts which are based on the publications or presentations of other authors, either in letter or in spirit, are specified as such in accordance with the citing guidelines. The sections on methodology (in particular regarding practical work, laboratory regulations, statistical processing) and results (in particular regarding figures, charts and tables) are exclusively my responsibility.

Furthermore, I declare that I have correctly marked all of the data, the analyses, and the conclusions generated from data obtained in collaboration with other persons, and that I have correctly marked my own contribution and the contributions of other persons (cf. declaration of contribution). I have correctly marked all texts or parts of texts that were generated in collaboration with other persons.

My contributions to any publications to this dissertation correspond to those stated in the below joint declaration made together with the supervisor. All publications created within the scope of the dissertation comply with the guidelines of the ICMJE (International Committee of Medical Journal Editors; http://www.icmje.org) on authorship. In addition, I declare that I shall comply with the regulations of Charité – Universitätsmedizin Berlin on ensuring good scientific practice.

I declare that I have not yet submitted this dissertation in identical or similar form to another Faculty.

The significance of this statutory declaration and the consequences of a false statutory declaration under criminal law (Sections 156, 161 of the German Criminal Code) are known to me.”

Date Signature

Declaration of your own contribution to the publications

Jan Roediger contributed the following to the below listed publications:

Publication 1: Jan Roediger, Till A. Dembek, Gregor Wenzel, Konstantin Butenko, Andrea A. Kühn, Andreas Horn, StimFit-A Data-Driven Algorithm for Automated Deep Brain Stimulation Programming, Movement Disorders, 2022

Contribution:
Jan Roediger conceptualized the study in consultation with his first and second supervisors Andrea Kühn and Andreas Horn. Together with Till Dembek he collected the training data at Cologne University Hospital within the scope of a previous studies.[11, 24] Using the Lead-DBS toolbox with helpful advice from Andreas Horn, Jan Roediger reconstructed DBS electrodes of all patients included in the study. He conceptualized, developed, and wrote the code for the StimFit algorithm as well as the scripts for data processing, statistical analysis, and visualization in consultation with Andreas Horn. Text, figures and accompanying material of the manuscript were written and designed by Jan Roediger and critically revised by all other authors.

Publication 2: Jan Roediger, Till A. Dembek, Johannes Achtzehn, Johannes L. Busch, Anna-Pauline Krämer, Katharina Faust, Gerd-Helge Schneider, Patricia Krause, Andreas Horn, Andrea A. Kühn, Automated Deep Brain Stimulation programming based on electrode location – a randomized, crossover trial using a data-driven algorithm, Lancet Digital Health, accepted

Contribution:
Jan Roediger conceptualized the study in consultation with his first and second supervisors Andrea Kühn and Andreas Horn as well as Till Dembek. He wrote and submitted the ethics proposal and - in collaboration with Andrea Kühn - acquired funding for the study. He recruited all patients that participated in the study and performed electrode reconstructions and data processing necessary in preparation for the study visits. Jan Roediger rated the patients motor performance during the study visit with assistance by Pauline Krämer, Johannes Achtzehn and Johannes Busch, who programmed the DBS devices. Jan Roediger conducted the statistical analysis and data visualization. He interpreted the results with help of Till Dembek and Andrea Kühn. Text, figures and accompanying material of the manuscript were written and designed by Jan Roediger and critically revised by all other authors.

_____

Signature, date and stamp of first supervising university professor / lecturer

_____

Signature of doctoral candidate

Publication I: StimFit-A Data-Driven Algorithm for Automated Deep Brain Stimulation Programming

Jan Roediger, Till A. Dembek, Gregor Wenzel, Konstantin Butenko, Andrea A. Kühn, Andreas Horn
DOI: https://doi.org/10.1002/mds.28878

Movement Disorders, 2021 - Rank 10 out of 208 journals for “Clinical Neurology” in 2020 (top 5%)

Journal Data Filtered By: **Selected JCR Year: 2020** Selected Editions: SCIE,SSCI
Selected Categories: **“CLINICAL NEUROLOGY”** Selected Category Scheme: WoS
Gesamtanzahl: 208 Journale

Rank	Full Journal Title	Total Cites	Journal Impact Factor	Eigenfactor Score
1	LANCET NEUROLOGY	43,457	44.182	0.059560
2	Nature Reviews Neurology	15,738	42.937	0.029580
3	Alzheimers & Dementia	21,824	21.566	0.045940
4	JAMA Neurology	17,086	18.302	0.043360
5	ACTA NEUROPATHOLOGICA	28,031	17.088	0.036970
6	BRAIN	64,627	13.501	0.061550
7	NEURO-ONCOLOGY	17,812	12.300	0.029210
8	SLEEP MEDICINE REVIEWS	11,218	11.609	0.014840
9	ANNALS OF NEUROLOGY	43,728	10.422	0.039960
10	MOVEMENT DISORDERS	35,072	10.338	0.030790
11	JOURNAL OF NEUROLOGY NEUROSURGERY AND PSYCHIATRY	37,094	10.154	0.026380
12	NEUROLOGY	109,905	9.910	0.097500
13	Brain Stimulation	9,206	8.955	0.015960
14	Neurology-Neuroimmunology & Neuroinflammation	3,863	8.485	0.008390
15	NEUROPATHOLOGY AND APPLIED NEUROBIOLOGY	4,791	8.090	0.004640
16	STROKE	78,912	7.914	0.068320
17	Neurotherapeutics	6,764	7.620	0.009400
18	NEUROSCIENTIST	5,949	7.519	0.005010
19	Epilepsy Currents	1,246	7.500	0.001750
20	JOURNAL OF HEADACHE AND PAIN	5,400	7.277	0.008140

Publication II: Automated Deep Brain Stimulation programming based on electrode location – a randomized, crossover trial using a data-driven algorithm

Jan Roediger, Till A. Dembek, Johannes Achtzehn, Johannes L. Busch, Anna-Pauline Krämer, Katharina Faust, Gerd-Helge Schneider, Patricia Krause, Andreas Horn, Andrea A. Kühn

DOI: https://doi.org/10.1016/S2589-7500(22)00214-X

Lancet Digital Health, accepted - Rank 1 out of 30 journals for “Medical Informatics” in 2020 (top 4%)

Journal Data Filtered By: **Selected JCR Year: 2020** Selected Editions: SCIE,SSCI
Selected Categories: **“MEDICAL INFORMATICS”**
Selected Category Scheme: WoS
Gesamtanzahl: 30 Journale

Rank	Full Journal Title	Total Cites	Journal Impact Factor	Eigenfactor Score
1	Lancet Digital Health	1,260	24.519	0.003000
2	npj Digital Medicine	2,406	11.653	0.007450
3	JOURNAL OF BIOMEDICAL INFORMATICS	12,255	6.317	0.014690
4	IEEE Journal of Biomedical and Health Informatics	7,850	5.772	0.012840
5	COMPUTER METHODS AND PROGRAMS IN BIOMEDICINE	12,277	5.428	0.011190
5	JOURNAL OF MEDICAL INTERNET RESEARCH	26,102	5.428	0.039100
7	ARTIFICIAL INTELLIGENCE IN MEDICINE	4,245	5.326	0.004220
8	JMIR mHealth and uHealth	7,694	4.773	0.015520
9	JOURNAL OF THE AMERICAN MEDICAL INFORMATICS ASSOCIATION	12,078	4.497	0.016910
10	JOURNAL OF MEDICAL SYSTEMS	8,017	4.460	0.009500
11	Internet Interventions-The Application of Information Technology in Mental and Behavioural Health	1,658	4.333	0.003310
12	JMIR Serious Games	641	4.143	0.000970
13	INTERNATIONAL JOURNAL OF MEDICAL INFORMATICS	7,651	4.046	0.010440
14	Digital Health	676	3.495	0.001640
15	Health Information Management Journal	541	3.185	0.000540
16	STATISTICAL METHODS IN MEDICAL RESEARCH	6,654	3.021	0.015730

Curriculum Vitae

Mein Lebenslauf wird aus datenschutzrechtlichen Gründen in der elektronischen Version meiner Arbeit nicht veröffentlicht

Acknowledgments

First and foremost, I would like to thank my supervisors Prof. Dr. Andrea Kühn and Dr. Andreas Horn for their support, advice, and trust during my PhD study. I would also like to thank Dr. Till Dembek and Prof. Dr. Lars Timmermann who, with their enthusiasm and knowledge inspired me to pursue this path. I further thank my colleagues and other friends, who with their kind help and encouragement had made these years rewarding and fruitful. Finally, my deep gratitude goes to my parents. Without their trust and support this would have been impossible.